



Norwegian University of
Science and Technology

Performance of a two-dimensional hydraulic model for the evaluation of stranding areas and characterization of rapid fluctuations in hydropeaking rivers

Storåne, Hallingdal

Ana Juárez

Hydropower Development

Submission date: June 2018

Supervisor: Knut Alfredsen, IBM

Co-supervisor: Ana Adeba Bustos, IBM

Norwegian University of Science and Technology
Department of Civil and Environmental Engineering



Norwegian University of
Science and Technology

Performance of a two-dimensional hydraulic model for the evaluation of stranding areas and characterization of rapid fluctuations in hydropeaking rivers

Storåne, Hallingdal

Ana Juárez Gómez

Hydropower Development

Submission date: June 2018

Supervisors: Knut Alfredsen, NTNU
Ana Adeva Bustos, NTNU

Norwegian University of Science and Technology
Department of Civil and Environmental Engineering

Preface

This thesis is submitted to the Norwegian University of Science and Technology (NTNU). It is a result of the course TVM4915 Hydropower Development, Master's Thesis (2018 VÅR). The topic of the thesis is the application of a 2D hydraulic model to assess environmental impact in hydropower rivers and characterization of the fluctuations.

The study was conducted at the Department of Civil and Environmental Engineering. I would like to express my gratefulness to my supervisors' professor Knut Alfredsen and PhD candidate Ana Adeva Bustos. Ana's encouragement has been essential for pushing my limits further. Thank you

The study was made possible in part by the cooperation with E-CO Energi, especially Bjørn Otto Dønnum, that supplied all needed data.

I would also like to thank:

- Morten Stickler for tips about analyzing and presenting results.
- Marcell Szabo-Meszaros for advice to process ADCP data.
- Rodrigo Suárez, for the all the advice, the experience, the Excel tips, the support, thanks for all.
- Javier, Kofi, Bendik, the HPD & Verkstadloftet for being part of this and making it a great experience.
- My parents who hesitated to support me in any decision I made.

Trondheim, June 18th, 2018

Ana Juárez Gómez

Abbreviations

ADCP – Acoustic Doppler Current Profiler

ALB – Airborne Laser Bathymetry

DTM – Digital Terrain Model

DEM – Digital Elevation Model

GPS – Global Positioning System

HEC-RAS – Hydrologic Engineering Center River Analysis System

LiDAR – Light Detection and Ranging

MDPI – Multidisciplinary Digital Publishing Institute

NVE – Norges Vassdrags- og Energidirektorat

NTNU – Norwegian University of Science and Technology

UTM – Universal Transverse Mercator

WFD – Water Framework Directive

WSE – Water Surface Elevation

Table of contents

| | |
|--|-----|
| Preface..... | ii |
| Abbreviations | iii |
| Table of contents | iv |
| Thesis structure | vi |
| 1. Introduction..... | 1 |
| 2. Methods..... | 2 |
| 2.1 Study site | 2 |
| 2.2 Characterization of rapid fluctuations | 3 |
| 2.3 Using LiDAR data for input geometry | 4 |
| 2.4 Scenarios..... | 4 |
| 2.5 Hydraulic model set up and calibration | 5 |
| Set up and calibration..... | 5 |
| Variation of wetted areas | 5 |
| Consideration of damping effect in dewatering velocity along the stream..... | 6 |
| Evaluation of dewatering velocity | 6 |
| 3. Results..... | 7 |
| 3.1 Characterization of flow and rapid fluctuations | 7 |
| Number of fluctuations | 7 |
| Discharge value at start and end of the fluctuations | 7 |
| Light conditions | 8 |
| Seasonal analysis | 8 |
| 3.2 Hydraulic model HEC-RAS | 8 |
| Calibration and model evaluation | 8 |
| Variation of wetted area..... | 10 |
| Consideration of damping effect in dewatering velocity along the stream..... | 11 |

| | |
|--|----|
| Dewatering speed..... | 15 |
| 4. Discussion | 17 |
| References | 18 |
| Appendix A COSH Tool extra figures Appendix A COSH Tool extra figures..... | 22 |
| Appendix B Model calibration..... | 24 |
| B.1 Comparison with Water edge from ALB survey | 24 |
| B.2 GPS Measurements..... | 25 |
| B.3 Low discharge calibration..... | 26 |
| B.4 Velocity comparison between model and field measurements..... | 27 |
| Appendix C Dried out map for different discharges and velocities..... | 29 |
| Appendix D Georeferenced pictures taken with drone in Storåne..... | 33 |
| Appendix E Consideration of damping effect..... | 35 |
| Appendix E Dewatering maps..... | 36 |
| Appendix F Field pictures | 39 |
| Appendix G Substrate distribution in Storåne..... | 43 |
| Appendix H Fish density..... | 45 |
| Appendix I Turbine restrictions | 47 |
| Hol I Operation limitations for the different turbines..... | 47 |
| Appendix J Cost of changing operation | 48 |
| Appendix K Gol, Hallingdal river..... | 49 |

Thesis structure

The thesis has an untraditional format in the sense that a paper is the main product. The paper is planned to be submitted to *Water*, an open access journal part of MDPI (Multidisciplinary Digital Publishing Institute).

A manuscript of the paper (“Performance of a two-dimensional hydraulic model for the evaluation of stranding areas and characterization of rapid fluctuations in hydropeaking rivers”) is therefore the main content of the thesis. Further information about the work, and results not included in the paper, are found in the appendixes.

Much of the thesis work was conducted using HEC-RAS 5.0.3, developed by the US Army Corps of Engineers and COSH Tool, a program created by SINTEF institute.

Performance of a two-dimensional hydraulic model for the evaluation of stranding areas and characterization of rapid fluctuations in hydropeaking rivers

Abstract: Extreme, short-duration fluctuations caused by hydropeaking occurs when hydropower is used to cover peaks for electrical loading conditions of the power network. Such a rapid dewatering processes may have a high impact for biological species, especially fish stranding. The present work analyzes these fluctuations using a two-dimensional unsteady model approach for quantification of two important hydro-morphological factors on fish stranding risk: the wetted area and the dewatering rate. This approach was applied on a 2-kilometer-long stream in Storåne, where topobathymetrical LiDAR data was available providing a high quality digital elevation model. Results show that the attenuation of the fluctuation due to the damping effect along the reach has a relevant role in assessing the dewatering speed. Moreover, the outcomes underline the need for mitigation in this area. We recommended an alternative scenario operation which combined with physical and biological data can help in decision making for developing constructive and morphological mitigation measurements.

Key words: Hydropeaking, HEC-RAS, 2D, COSH Tool, modelling.

1. Introduction

By 2050, the EU should cut greenhouse gas emissions to 80% below 1990 levels (European Commission, 2018). The power sector has the biggest potential for cutting emissions and therefore energy transition is a fundamental step towards sustainability. In this frame, hydropower is expected to play a key role to balance the load of other renewable resources. Norway has approximately half of the hydropower reservoir capacity in Europe (Ingeborg Graabak, 2017). Short-term changes in electricity demands, for instance because of stochastic electricity generation from solar and wind energy, will increase hydropeaking production leading to higher fluctuations in discharge and water levels.

In addition, the implementation of the Water framework Directive and the revision of hydropower licenses in Norway in 2022 (NVE, 2018) may lead to new environmental restrictions in regulated rivers. Consequently, information for decision making is necessary.

Ecological impacts of hydropeaking have been reviewed by Harby, Alfredsen, Fjeldstad, & Halleraker, 2001; Cushman, 1985. Among the most important impacts are the drifting of macroinvertebrates (Lauters, Lavandier, Lim, & Belaud, 1996) and the stranding of juvenile fish. Fish stranding is produced whenever fish are restricted to poor habitat due to physical separation from a main body of water because of flow decrease (Nagrodski, Raby, Hasler, Taylor, & Cooke, 2012). There are several studies on fish stranding produced by hydropeaking (Bradford, 1998; T. Vehanen, 2000; Salveit, Halleraker, Arnekleiv, & Harby, 2001; G. Berland, 2004; Flodmark, Vøllestad, & Forseth, 2004; Stillwater Sciences, 2006). They indicate how river morphology can affect the stranding of juvenile salmon and trout. These species, unable to follow the recessive water line when rapid decrease occurs, may strand on flat river banks or be trapped in pools disconnected from the main channel which are gradually dewatered. Although fish stranding experiments have been performed in laboratories (Bradford, 1998; Halleraker J. H., 2003) or in limited areas in rivers (Salveit, Halleraker, Arnekleiv, & Harby, 2001), very few studies exist on a larger scale in rivers about stranding. Therefore, there are not many guidelines for the assessment of impacts of peaking operation on fish mortality.

Stranding of fish and its mitigation are fundamental issues in the study of hydropeaking power plants and consequently they should be included in the revision of licenses in Norway in 2022. These studies should include measures to avoid and/or mitigate stranding. Hydraulic modelling has become a powerful tool in the assessment of river impacts. A two-dimensional model was applied in the case-study Lundesokna River to assess the stranding fish (Vanzo, Siviglia, Giido, Alfredsen, & Tancon, 2016;

Tuhtan, Noack, & Wieprecht, 2011); 2D-modelling has also been used to study habitat simulation (Choi, Kim, Choi, & Kim, 2017).

There are three principal methods to reduce hydropower impacts. The first one is *operational* measures, which focus on changing the performance of energy production, for example by imposing a minimum flow or changing the time operation of the turbines (Yin, Yang, & Petts, 2012) with the consequence of reducing benefits by the HPP operator (Gostner, Lucarelli, Theiner, Krager, & Schleiss, 2011). The second one is *constructive* measures that decrease the hydropeaking flows downstream the outlet by building dikes, basins, bypass tunnels or other structures but with high investment costs. Finally, *morphological* measures, that aim to restore a good level of naturalness of the river with a consequent improvement of the area suitable for the biotic system. Recent studies show that the best choice of intervention the proper mix of morphological, operational and constructive measures to minimize ratio between investment costs and ecological benefits (Gostner, Lucarelli, Theiner, Krager, & Schleiss, 2011; Adeva Bustos, et al., 2017).

Modeling and quantification of ecological effect of hydropeaking interactions are a main issue to select appropriate mitigation methods. For instance, different river management guidelines indicate suitable ranges of wetted area variation and dewatering rate to diminish the stranding risk like the Handbook for environmental design in regulated salmon rivers (Bakken, Forseth, & Harby, 2016).

The aim of this paper is to assess the stranding risk based on two main hydro-morphological features: wetted area and dewatering velocity. For that, we propose an approach based on characterization of the fluctuations and a 2D hydraulic model. The model investigation focuses on the case study of Storåne River (Norway), where the fish community (brown trout) is strongly threatened by the hydro-morphological impacts of the hydropower production of Hol I hydropower plant. We simulate 6 different simplified scenarios of the current operation and alternative operation to investigate the dewatering phase (or recession phase). We evaluate the variation of wetted area and the dewatering rates based on the guidelines provided in the Handbook for Environmental Design River previously mentioned to identify the least harmful dewatering scenario for the considered configurations. The input geomorphology is based on LiDAR data (Airborne Light Detection and Ranging) a remote sensing technique for mapping shallow water bodies which is increasingly used for topo bathymetric surveys providing a high quality digital elevation model (Alne, 2016).

The results from this work will help improve current available guidelines on the procedure to assess environmental impact in hydropeaking rivers, specifically if existing LiDAR data is provided. This will also contribute in the decision making for mitigation measures in the study area.

2. Methods

2.1 Study site

The area of study is part of the river Storåne, located in Hol Municipality in Hallingdal in Buskerud county in Norway. It is a part of E-CO Energi's regulation. The study area is from the outlet of the power plant Hol 1 to Hovsfjorden (Figure 1 & Appendix F). The first 400 meters is a manmade stone laid trapezoidal channel whereas the rest of the river has natural bends and formations with several side streams, forming three main islands: Ellingøyne, Gjerdegøyne and Mørkaøyne. The bank widths range from 10 - 150 meters. The discharge depends on the production in Hol 1 in addition to the unregulated bypassed section, which catchment areas are 725 km² and 163 km² respectively (E-co 100% Ren Energi, 2018). Storåne is a clear, relatively shallow (mean < 1 m) mountain stream. The mesohabitat varies between glide and riffle with some steep sections. The river bed mainly consists of cobbles with an increasing amount of gravel in the lower part (Bendiksbj, 2013)(Appendix G).

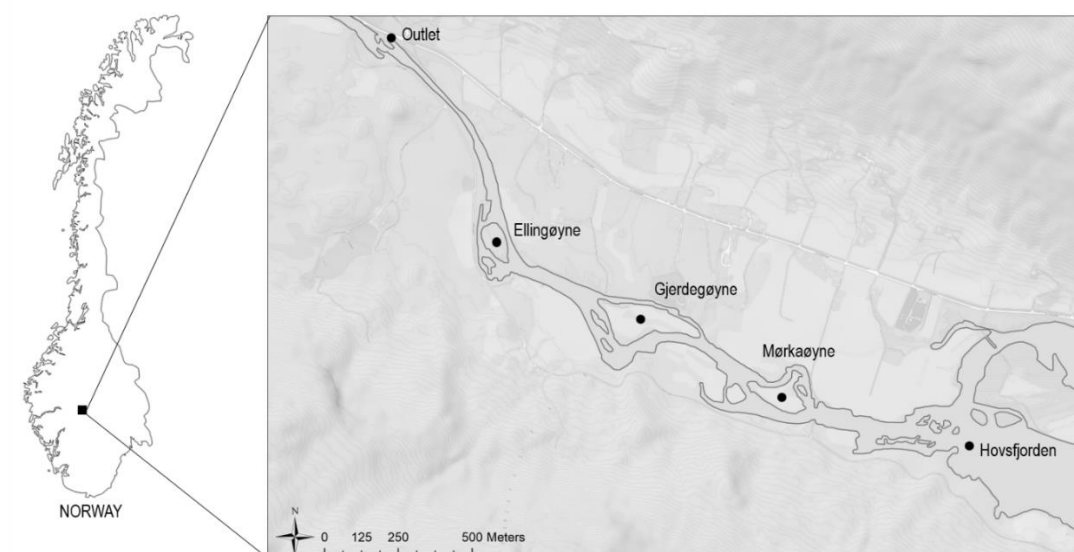


Figure 1 Illustration of Storåne river location in Norway and location of the selected study area from the outlet Hol I hydropower plant to Hovsfjorden with the formations around the 3 main islands: Ellingøyne, Gjerdegøyne and Mørkaøyne.

2.2 Characterization of rapid fluctuations

The characterization of the peaking events was made by COSH-Tool. It is a computational tool designed to quantify rapid fluctuations of flow in hydropeaking rivers (Julian Friedrich Sauterleute, 2014). In contrast with other similar analyses, it separates peaking events into rapid increases and rapid decreases (Figure A1). It also analyses daylight conditions during peaking events and calculates the parameters for a specific season of the year defined by the user (Julian Friedrich Sauterleute, 2014). The tool characterizes the fluctuations in flow based on three parameters: magnitude, time and frequency. Discharge data is needed as an input for the program.

E-CO Energi provided time series of discharge every 5 minutes from 2010 to 2017. The station is located 100 meters downstream the outlet and it measures the flow through Hol I power station plus the base flow from Storåne. Three floods were found in the data series in 2010, 2011 and 2015 (Figure 2). The maximum discharge released by the turbines is $60 \text{ m}^3/\text{s}$ (Dønnum, 2016), and therefore these events were not considered for the characterization of the rapid fluctuations since they are a result of heavy rainfall events.

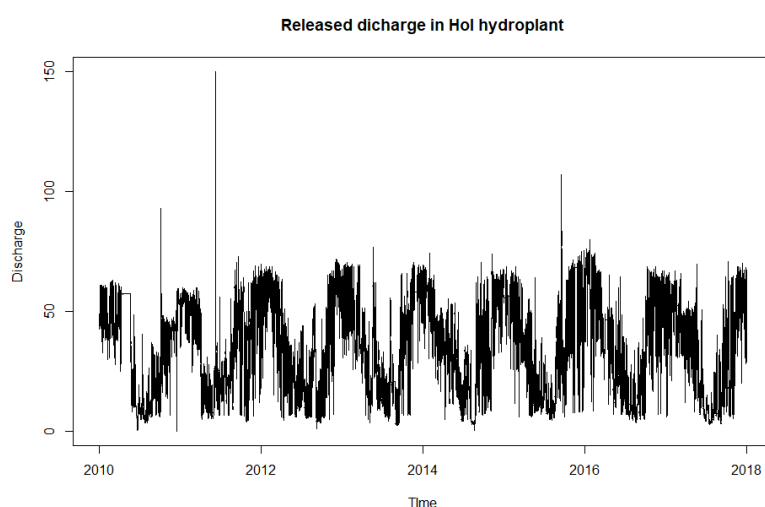


Figure 2. Flow data measured downstream of Hol I hydropower station from 2010 to 2017

2.3 Using LiDAR data for input geometry

As an input for the 2D hydraulic model, geometry data was collected along the river reach by an Airborne Laser Bathymetry (ALB) survey providing high resolution Airborne Light Detection and Ranging data (LiDAR). ALB is a remote sensing technique for mapping shallow water bodies (<10 m) which is increasingly used for topobathymetric surveys. ALB is a fast method for collecting data with a high density, covering rivers of 15-20 km in few hours. The high level of detail results in a large amount of data, which requires extensive processing before it can be used. The data was delivered as LAZ files, that had to be decompressed to LAS files. Later we imported it to a Geographic Information System (ArcMap) to create the Digital Elevation Model (DEM) that can be used as an input in the hydraulic model.

The entire length of the study site from the outlet to Hovsfjord is 2 km. The data was collected along a 2.6 km length that included also part upstream and downstream of the study site. The number of points recorded were more than 82 million with an accuracy of 6 cm in the XY plane and mean error of 3 cm in Z axis (Alne, 2016). This data set provided a high enough point density to create a DEM with a resolution of 0.5 m.

2.4 Scenarios

A series of different turbine shut down scenarios have been designed to simulate and quantify the stranding risk areas downstream Hol I power plant. The station has four turbines, each one with a capacity of 15 m³/s. The base flow was set at 6 m³/s representing the 5-percentile flow (Table 4).

Currently the typical dewatering scenario is a discharge decrease of 15m³/s in 5 minutes for each turbine. This configuration represents the Scenarios A. There are three different scenarios A: A10, the power plant decreases the production from 1 turbine (21m³/s) to base flow (6m³/s); scenario A21, the power plant decreases the production from 2 turbines (36m³/s) to 1 turbine (21 m³/s) and scenario A32, the discharge falls from 3 turbines (51m³/s) to 2 turbines (36m³/s) (Figure 4). The 4 turbines (66m³/s) scenario has been considered for the wetted areas but not for dewatering scenarios since it goes over the 95-percentile discharge and therefore is not so critical for stranding impact.

All the possible scenarios combinations can be obtained by overlapping the simplified scenarios that are proposed in the previous paragraph, for instance, dewatering velocity when going from 3 to 0 turbines in 5 minutes will be obtain by overlapping scenarios A32, A21 & A10.

We design a different alternative for each of these scenarios, called Scenarios B. Scenario B10 consist of decreasing from 1 turbine to 0 turbines increasing the stopping time from 5 minutes to 30 minutes. The first part would decrease the discharge from 100% down to 40% of the turbine capacity in 25 minutes before the turbine is completely stopped. This is due to the manufacturer restrictions, turbines cannot operate at values under 40% of max discharge (Dønnum, 2016). The scenarios B21 and B32 would be analogous to scenario B10 but with the corresponding turbines.

Changing the operation of the turbines will reduce the benefit for the HPP operator. The cost of this mitigation measure is calculated in Appendix J.

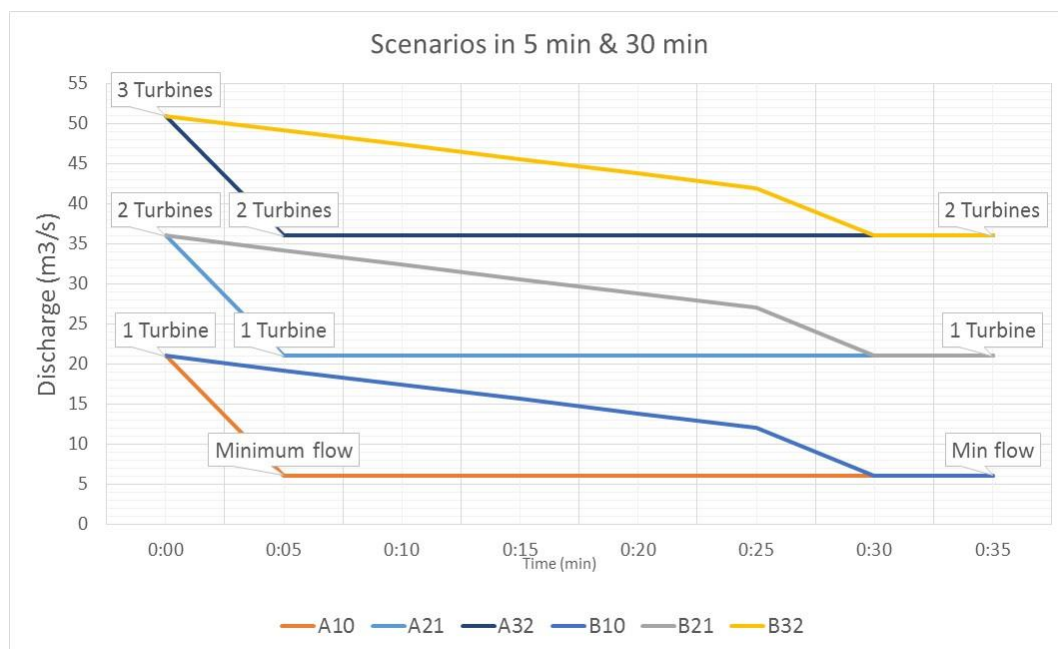


Figure 3. Dewatering scenarios for stranding risk modeling in Storåne river

2.5 Hydraulic model set up and calibration

Set up and calibration

The HEC-RAS 5.0.3. (USACE, 2018) computer program was used for the simulations with an equation set of diffusion wave. The Manning n was set by default at 0.06. The input geometry was the DEM with 1-meter resolution in the stream and 0.25-meter resolution in the river banks and singular points.

Calibration was made by using three main data resources covering a discharge from 2.44 to 44.72 m^3/s . The sources used were the water edge provided from LiDAR company; GPS measurements along the water edge and comparison with pictures from Norge i Bilder. Additionally ADCP measurements in two different profiles were taken to check velocity simulations.

The comparison with the water edge from ALB survey was made visually as a first approach to check the model performance. We analyze with a steady simulation of 31.72 m^3/s , that was the discharge according to the LiDAR company the day of the flight. However, this might slightly differ due to variations in discharge along the day (see Appendix B.1).

The comparison with GPS measurement followed a more analytical procedure. The points were recorded during 2 consecutive days, September 19th and 20th, at different hours. The discharge suffered slight fluctuations during the day and therefore the points were grouped in 4 sections depending on time and day (see Appendix B.2). We did a steady simulation for every discharge, imported the obtained Water Surface Elevation (WSE) from HEC-RAS into ArcMap and extracted in the measured points the elevation obtained in the simulation. We compare the simulated WSE against measured WSE to evaluate the accuracy of the model.

Finally, to obtain a broader range of discharge for comparison we selected a picture from Norge I Bilder from 2006 with a recorded discharge of 2.44 m^3/s . The calibration is made visually by comparing the wetted areas and water edge in the picture with the simulation (see Appendix B.3).

Variation of wetted areas

The maximum potential stranding area are those which get dry when passing from high to low flow. We run steady simulations for the discharges considered in the different scenarios at 66, 51, 36, 27, 21, 12 and 6 m^3/s . For each of these flows we calculate the wetted area. The dried-out area is calculated taken as a reference 66 m^3/s as full covered wetted area. These areas are also represented in different

maps representing dried areas depending on the number of turbines that are on at the start and at the end of the scenario.

1,4 turbines represent the middle step of scenario B21, when there is one turbine working and another one at its 40% capacity (see Figure 3 Scenario B21). Correspondingly 0.4 represents the middle step of scenario B10, when there is only one turbine working at its 40% capacity.

We also calculated the dried-out area for every cubic meter per second of flow reduced to have a ratio of the impact of decreasing the flow.

$$Dried\ out\ area_i \left(\frac{m^2}{\frac{m^3}{s}} \right) = \frac{\frac{Dried\ area_i}{Dried\ area_{i-1}}}{Reduced\ discharge_i}$$

Equation 1 Calculation of marginal dried out area (m²) per unit of flow (m³/s)

Consideration of damping effect in dewatering velocity along the stream

The damping effect is a decrease in the amplitude of an oscillation because of energy being drained from the system to overcome frictional or other resistive forces. In our case when the turbine is shut down it creates a wave which will be steep and marked right after the outlet but will be smoother and longer the more downstream it is. This is a factor we need to consider when calculating the dewatering velocity ratio.

A simulation of 3 hours of duration was run to enable the evaluation of the damping effect. In the first 5 minutes the discharge changes from 66 m³/s (4 turbines plus base flow) to 6 m³/s (base flow).

We generate Water Surface Elevation (WSE) maps every 5 minutes, a total of 35 WSE maps at different times. The maps were computed in HEC-RAS and imported into ArcMap. For each map we extract in 10 different points the WSE and evaluate the damping effect.

Evaluation of dewatering velocity

Stranding of juvenile fish has been a documented consequence below hydropeaking power stations. Ramping rates should not be higher than 10 cm/h to reduce stranding of fish (Halleraker J. H., 2003).

The Center for Environmental Design of Renewable Energy (CEDREN) designed some indexes to assess the impact of dewatering velocity in rivers (Bakken , Forseth, & Harby, 2016). In our study, the dewatering velocity is defined as the critical velocity recorded during an episode with a 5 minutes time resolution.

Table 1. Dewatering velocity rates (with color code) to assess the impact of hydropeaking according to the Handbook for Environmental design in regulated Salmon Rivers (Bakken , Forseth, & Harby, 2016)

| Impact | Dewatering velocity (cm/h) |
|----------|----------------------------|
| Very big | >20 |
| Big | 13-20 |
| Moderate | 5-10 |
| Small | <5 |

The dewatering maps for each scenario are created with both WSE at start and end of the scenario divided by the time in which the wave is produced. Notice that this time is not the same in every point due to the damping effect and therefore we need a raster map in which every point has a different duration depending on the distance to the outlet.

3. Results

3.1 Characterization of flow and rapid fluctuations

The mean flow downstream Hol I hydropower plant is 35.88 m³/s. The minimum flow recorded was 0.05 m³/s in August 8th, 2014 while the maximum flow was 150.08 m³/s in September 6th, 2011. Notice that the 5-percentile discharge (6m³/s) and the 95-percentile discharge (64m³/s) correspond with the minimum and maximum discharges in the modelled scenarios.

Table 2. Descriptive statistics of flow data from 2010 to 2017 downstream of Hol I hydropower plant.

| Parameter | Discharge (m ³ /s) |
|---------------|-------------------------------|
| Min flow | 0.05 |
| 5-percentile | 6.12 |
| 10-percentil | 8.62 |
| Mean flow | 35.88 |
| 90-percentile | 61.10 |
| 95-percentile | 64.17 |
| Max flow | 150.08 |

Number of fluctuations

The number of increases and decreases per year is above 300 since 2012 as can be seen in Figure 4.

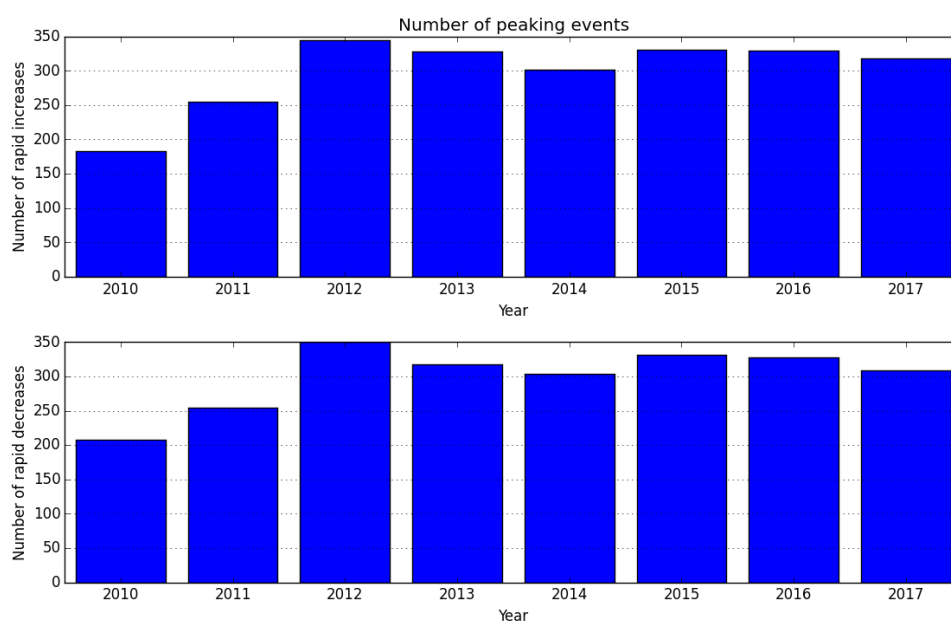


Figure 4. Number of peaking events per year in Hol I hydro plant.

Discharge value at start and end of the fluctuations

Most of the rapid increase started at a relatively high discharges (mean 43 m³/s). Correspondingly, most of the rapid decreases stopped at relatively high discharges (median 34.61 m³/s). However, 25% of this fluctuation limits are below 18.7 m³/s and 10% are below 9 m³/s (Figure & Table 3).

Table 3. Descriptive statistics for the discharge at the start of an increase and the end of a decrease in the period 2010 to 2017 downstream Hol I hydropower plant.

| | Start | End |
|-----------------------------------|-------------------|-------------------|
| 2010-2017 | Increases | Decreases |
| | m ³ /s | m ³ /s |
| Minimum | 2.38 | 0.05 |
| 10th-Percentile | 8.98 | 8.74 |
| 25th-Percentil | 18.78 | 18.72 |
| Mean | 34.04 | 33.71 |
| Median | 34.52 | 34.61 |
| 75th-Percentil | 47.38 | 46.81 |
| 90th-Percentile | 56.8 | 56.15 |
| Maximum | 100.51 | 95.85 |
| Standard dev | 17.08 | 16.69 |

Light conditions

According to (Halleraker J. H., 2003) it is recommended to dewater in darkness all year to reduce stranding of fish. In Storåne, most of the rapid increases occur during daylight (71%) while most of the rapid decreases occur during darkness (70%), see Table 4. This pattern is the same during the winter season (Appendix A).

Table 4. Percentage of Increases and Decreases during daylight, twilight and darkness.

| | Increase peaks | Decrease peaks |
|-----------------|-----------------------|-----------------------|
| Daylight | 71% | 29% |
| Twilight | 0% | 1% |
| Darkness | 29% | 70% |

Seasonal analysis

A far higher incidence of fish stranding occurs during winter conditions (<4.5 °C) compared with the higher temperatures during late summer and early autumn (Salveit, Halleraker, Arnekleiv, & Harby, 2001; Person, 2013). However in Storåne the pattern during winter season is similar to the entire year (Figure A3 & A4).

3.2 Hydraulic model HEC-RAS

Calibration and model evaluation

The HEC-RAS simulations for different discharges in Storåne river were calibrated with good accuracy for the default Manning of 0.06 m. Other Manning numbers were tested with no relevant changes in the model response. A total of 253 GPS points were compared with the model giving a mean error of 6 cm and a standard deviation of 6 cm (Figure 5.cI).

The comparison with the water edge of the ALB survey flight and the Norge I Bilder picture were very similar to the model simulation for the corresponding discharges (31.72 & 2.44 m³/s) as can be seen in Figure 5 a,b & Appendix B Figure B1). It is worth noting that including the Norge I Bilder picture taken with 2.44 m³/s the lowest discharge values are covered, representing the zero-production with minimum flow coming from the river upstream.

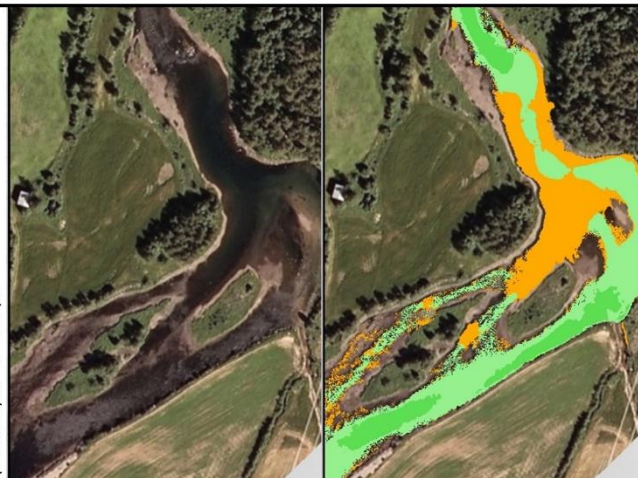
Two velocity profile measurements were also carried out, one in Gjerdeøyne and the other in Mørkeøyne. The first one obtained good results with an R²=0.77 (Figure 5.dI) and a similar profile distribution (Figure 5.dII). Mørkeøyne profile can be seen in Appendix B.

VISUAL COMPARISON

a) Comparison of model simulation with water edge recorded the day of the flight (Red) Q=31.72 m³/s



b) Comparison Norge I Bilder (Top), Norge I Bilder picture with model for 2.44 m³/s overlapped (Bottom) Q= 2.44 m³/s



GPS POINTS CALIBRATION

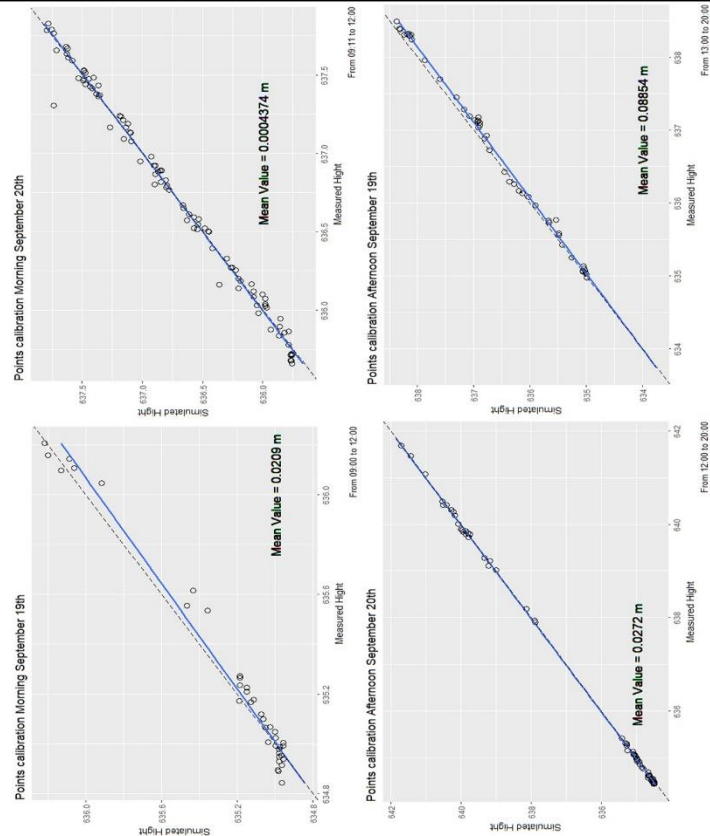
c.i) Absolute error descriptive statistics (all in m) for the GPS point compared

| Total number of points | 253 | Discharge (m ³ /s) |
|------------------------|------|-------------------------------|
| Minimum | 0.00 | 44.72 |
| 25th percentile | 0.02 | 43.82 |
| Mean error | 0.06 | 15.70 |
| 75th percentile | 0.07 | 15.48 |
| Maximum | 0.43 | |
| Standard deviation | 0.06 | |

c.ii) Model calibration points groups, for different day, time and discharge

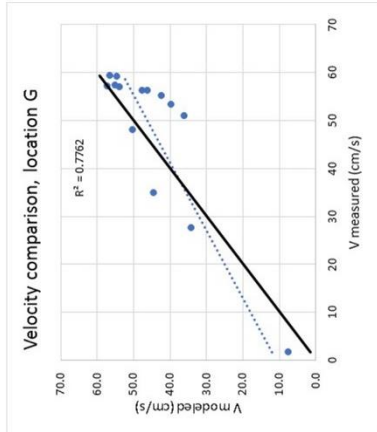
| Day | Daytime | Discharge (m ³ /s) |
|--------|-----------|-------------------------------|
| 19-Sep | Morning | 44.72 |
| 19-Sep | Afternoon | 43.82 |
| 20-Sep | Morning | 15.70 |
| 20-Sep | Afternoon | 15.48 |

c.iii) Calibration: simulated against measured water levels; blue continuous line represents the linear regression. Discharge indicated in table c.ii, in the range from 15.48 to 44.72 m³/s



VELOCITY COMPARISON

d.i) Velocity comparison. Measured velocity against modeled velocity. R²=0.7762



d.ii) Velocity comparison. Measured velocity profile and modeled velocity profile.

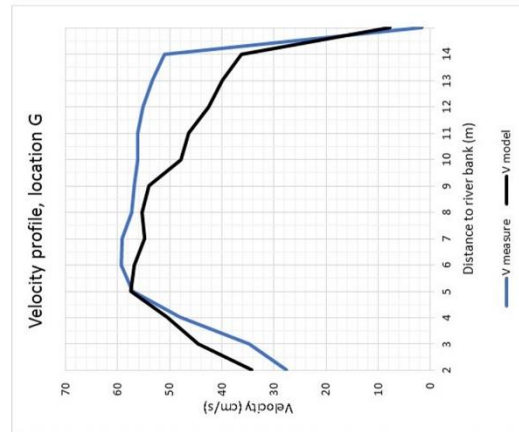


Figure 5. Calibration: a) Comparison with LiDAR water edge; b) Comparison with Norge I Bilder picture; c) GPS points calibration & d) Velocity comparison

Variation of wetted area

In the investigated area, our simulations return a wetted area of 260593 m² under full production conditions against 169667 m² under base flow conditions. We consider 4 turbines functioning plus base flow (66 m³/s) as a reference of full covered wetted area. When we go from 4 turbines working to 3 turbines working the area reduced is 4%; from 3 turbines to 2 turbines the area reduced is 11%; with only 1 turbine working (21 m³/s) the dried-out area is 18% and with no production and base flow (6m³/s) the dried-out area reaches 35% (Table 5).

The calculations on dried-out area per cubic meter of reduced discharge are shown in Table. The table shows that when discharge is between 66 & 51 m³/s a reduction of 1 m³/s will mean around 753 m². In contrast when discharge is 6 m³/s a reduction of 1 m³/s will dry 4848 m² (6.4 times more). It is worth noticing that there is a clear increase in the dried-out area for flows between 21 and 12 m³/s (1523 m²) and even more accentuated for flows between 12 and 6 m³/s, where a decrease of 1 m³/s is equivalent to a 4848 m² of dried out area.

Table 5. Number of turbines on for different scenarios, its correspondent discharge and reduced discharge, the wetted area associated, dried out area, percentage of dried out area and marginal dried out area per reduced discharge.

| Turbines | Discharge (m ³ /s) | Reduced discharge (m ³ /s) | Wetted area (m ²) | Dried out area (m ²) | Dried out area (%) | Dried out area(m ²)/ Reduced discharge (m ³ /s) |
|----------|-------------------------------|---------------------------------------|-------------------------------|----------------------------------|--------------------|--|
| 4 | 66 | 0 | 260593 | 0 | 0% | 0 |
| 3 | 51 | 15 | 249293 | 11300 | 4% | 753 |
| 2 | 36 | 15 | 230668 | 29925 | 11% | 1242 |
| 1.4 | 27 | 9 | 218982 | 41611 | 16% | 1298 |
| 1 | 21 | 6 | 212461 | 48132 | 18% | 1087 |
| 0.4 | 12 | 9 | 198756 | 61837 | 24% | 1523 |
| 0 | 6 | 6 | 169667 | 90926 | 35% | 4848 |

We represented the dried-out areas for different discharges and scenarios that can be seen in Appendix C. It is important to mention that the model calibration showed an accuracy of 6 cm, therefore when depth is below this value we cannot be certain whether the area is wetted or not.

Some streams are especially affected by base flow conditions. The water in the western stream in Ellingøyne is almost completely dried off and stagnant, with velocity below 0.05 m/s (Figure 6), this occur mainly when flow is lower than 21 m³/s (Figure C2). Notice than in this area stranding fish has been observed (Stickler, 2018).

At base flow, the northern stream in Gjerdeøyne is also dried out and almost motionless with very low velocity in the areas where there is some water left, this occurs mainly for flow lower than 21 m³/s. The southern stream in Gjerdeøyne also has big dried areas. These dried areas are more evenly distributed, meaning that they start drying when flow starts decreasing in a smoother way.

The northern stream in Mørkaøyne and the south-occidental stream show big dried areas also with motionless water.

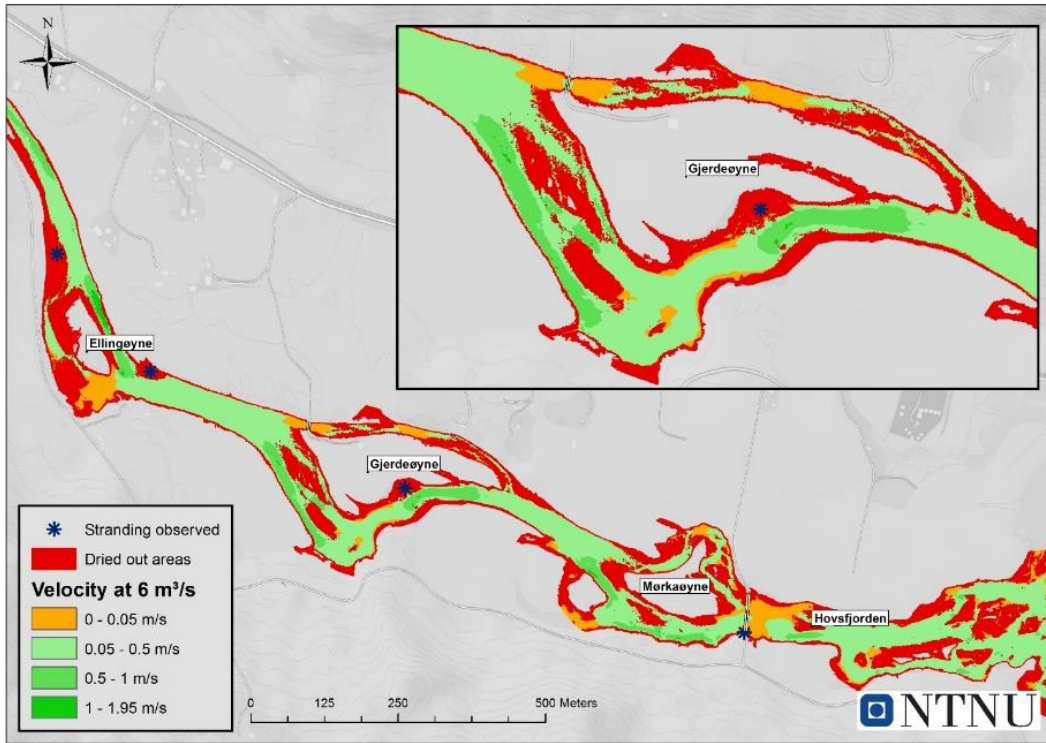


Figure 6. Variation of wetted area downstream Hol I hydropower plant: in green the velocity of wetted at base flow, in red the area dried passing from 51 m³/s to base flow (6m³/s)

Consideration of damping effect in dewatering velocity along the stream

The results show that there is a clear wave attenuation along the stream in Storåne. When changing the hydropower flow from 66 to 6 m³/s in 5 minutes, the duration of the wave will be longer the further downstream. Points shown in Figure 7 from 1 to 10 are the main points to study the wave propagation.

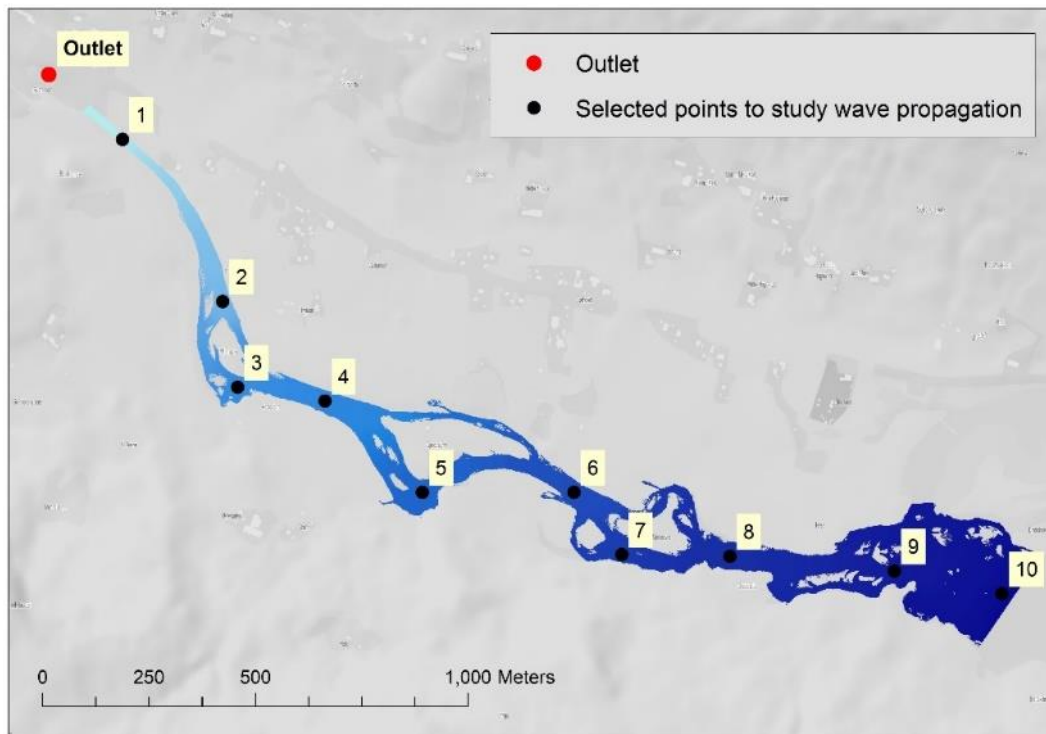


Figure 7 Points along Storåne river where WSE was extracted to evaluate the damping effect along the reach. Points from 1 to 10 are the main selected points to study wave propagation.

The wave expansion can be clearly observed in Table 6. The table displays all Water Surface Elevation for the representative points every five minutes. In point 1 the WSE changes from 642.34 m to 640.91 m within 10 minutes producing the sharpest change in minute 15; in point 3, located in Ellingøyne, the WSE changes from 638.63 m to 637.64 m within 45 minutes, producing the sharpest change in minute 25; in point 5 located in Gjerdeøyne the WSE changes from 637.16 m to 636.22 m in 65 minutes with the sharpest change in minute 30; in point 8 located downstream Mørkaøyne WSE changes from 635.20 m to 634.21 m in 1 hour and 30 minutes with the sharpest change in minute 40.

In contrast we run a simulation with the alternative operation procedure, scenarios B43, B32, 321 & B10, shutting down all the turbines in 2 hours instead of in 5 minutes. In table 8 we can see that the wave is broader. For example, in point 3, the wave is produced in a total of 3 hours instead of 45 minutes, in point 5 located in Gjerdeøyne the wave is produced 3:30 hours instead of 2:05 hours and in point 8 in Mørkaøyne the wave is produced in 4:15 hours instead of 1:25 hours. Notice that in point 1 we still find some WSE decrease over 10 cm at 1:10, 1:40 & 2:10, these are the consequence of stopping the last 40% capacities of the turbines in 5 minutes which induce a higher wave that cannot be mitigate changing operation of the turbines.

The colors show the rate of change for every step: if there is no change in WSE it is shown in grey; if change is between 0 and 2 cm the color is light yellow; if change is between 2 and 5 cm the color is light pink; change between 5 and 10 cm is shown in green and change higher than 10 cm is shown in red.

Table 6. Water Surface Elevation (WSE) for the 10 selected points along Storåne after a discharge variation from 66 to 6 m³/s in 5 minutes (current possible operation).

| Time | Point 1 | Point 2 | Point 3 | Point 4 | Point 5 | Point 6 | Point 7 | Point 8 | Point 9 | Point 10 |
|------|---------|---------|---------|---------|---------|---------|---------|---------|---------|----------|
| 0:05 | 642.34 | 640.12 | 638.63 | 638.35 | 637.16 | 636.24 | 635.65 | 635.2 | 634.34 | 633.75 |
| 0:10 | 641.45 | 640.03 | 638.6 | 638.34 | 637.16 | 636.24 | 635.65 | 635.2 | 634.34 | 633.75 |
| 0:15 | 640.93 | 639.76 | 638.36 | 638.19 | 637.12 | 636.23 | 635.65 | 635.2 | 634.34 | 633.75 |
| 0:20 | 640.91 | 639.61 | 638.06 | 637.96 | 636.95 | 636.16 | 635.61 | 635.18 | 634.34 | 633.75 |
| 0:25 | 640.91 | 639.54 | 637.87 | 637.8 | 636.73 | 636.02 | 635.5 | 635.12 | 634.33 | 633.75 |
| 0:30 | 640.91 | 639.52 | 637.77 | 637.71 | 636.55 | 635.86 | 635.36 | 635 | 634.29 | 633.73 |
| 0:35 | 640.91 | 639.51 | 637.71 | 637.66 | 636.42 | 635.74 | 635.21 | 634.87 | 634.23 | 633.71 |
| 0:40 | 640.91 | 639.51 | 637.68 | 637.63 | 636.34 | 635.66 | 635.09 | 634.75 | 634.16 | 633.68 |
| 0:45 | 640.91 | 639.5 | 637.66 | 637.61 | 636.3 | 635.6 | 635 | 634.63 | 634.09 | 633.64 |
| 0:50 | 640.91 | 639.5 | 637.65 | 637.6 | 636.27 | 635.56 | 634.94 | 634.53 | 634.03 | 633.61 |
| 0:55 | 640.91 | 639.5 | 637.64 | 637.59 | 636.25 | 635.53 | 634.9 | 634.46 | 633.98 | 633.58 |
| 1:00 | 640.91 | 639.5 | 637.64 | 637.59 | 636.24 | 635.51 | 634.87 | 634.4 | 633.93 | 633.55 |
| 1:05 | 640.91 | 639.5 | 637.64 | 637.59 | 636.23 | 635.5 | 634.84 | 634.35 | 633.9 | 633.52 |
| 1:10 | 640.91 | 639.5 | 637.64 | 637.59 | 636.23 | 635.5 | 634.83 | 634.31 | 633.87 | 633.5 |
| 1:15 | 640.91 | 639.5 | 637.64 | 637.59 | 636.23 | 635.49 | 634.82 | 634.28 | 633.85 | 633.48 |
| 1:20 | 640.91 | 639.5 | 637.64 | 637.58 | 636.22 | 635.49 | 634.82 | 634.26 | 633.83 | 633.47 |
| 1:25 | 640.91 | 639.5 | 637.64 | 637.58 | 636.22 | 635.49 | 634.81 | 634.25 | 633.81 | 633.45 |
| 1:30 | 640.91 | 639.5 | 637.64 | 637.58 | 636.22 | 635.49 | 634.81 | 634.24 | 633.8 | 633.44 |
| 1:35 | 640.91 | 639.5 | 637.64 | 637.58 | 636.22 | 635.49 | 634.81 | 634.23 | 633.79 | 633.43 |
| 1:40 | 640.91 | 639.5 | 637.64 | 637.58 | 636.22 | 635.48 | 634.81 | 634.22 | 633.79 | 633.42 |
| 1:45 | 640.91 | 639.5 | 637.64 | 637.58 | 636.22 | 635.48 | 634.81 | 634.22 | 633.78 | 633.41 |
| 1:50 | 640.91 | 639.5 | 637.64 | 637.58 | 636.22 | 635.48 | 634.81 | 634.21 | 633.78 | 633.41 |
| 1:55 | 640.91 | 639.5 | 637.64 | 637.58 | 636.22 | 635.48 | 634.81 | 634.21 | 633.78 | 633.4 |
| 2:00 | 640.91 | 639.5 | 637.64 | 637.58 | 636.22 | 635.48 | 634.81 | 634.21 | 633.78 | 633.4 |
| 2:05 | 640.91 | 639.5 | 637.64 | 637.58 | 636.22 | 635.48 | 634.81 | 634.21 | 633.77 | 633.4 |
| 2:10 | 640.91 | 639.5 | 637.64 | 637.58 | 636.22 | 635.48 | 634.81 | 634.21 | 633.77 | 633.39 |
| 2:15 | 640.91 | 639.5 | 637.64 | 637.58 | 636.22 | 635.48 | 634.81 | 634.21 | 633.77 | 633.39 |
| 2:20 | 640.91 | 639.5 | 637.64 | 637.58 | 636.22 | 635.48 | 634.81 | 634.21 | 633.77 | 633.39 |
| 2:25 | 640.91 | 639.5 | 637.64 | 637.58 | 636.22 | 635.48 | 634.81 | 634.21 | 633.77 | 633.39 |
| 2:30 | 640.91 | 639.5 | 637.64 | 637.58 | 636.22 | 635.48 | 634.81 | 634.21 | 633.77 | 633.39 |
| 2:35 | 640.91 | 639.5 | 637.64 | 637.58 | 636.22 | 635.48 | 634.81 | 634.21 | 633.77 | 633.39 |
| 2:40 | 640.91 | 639.5 | 637.64 | 637.58 | 636.22 | 635.48 | 634.81 | 634.21 | 633.77 | 633.39 |

Table 7. Color legend of the WSE decrease every step (5min) in the considered scenario.







| Color | WSE decrease (cm) |
|---|-------------------|
|  | None |
|  | 0-2 |
|  | 2-5 |
|  | 5-10 |
|  | >10 |
|  | Max |

Table 8. WSE for the 10 selected points along Storåne after a discharge variation from 66 to 6 m³/s following the proposed scenarios B43, B32, B21 & B10.

| Time | 1 | 2 | 3 | 4 | 5 | 6 | 7 | 8 | 9 | 10 |
|------|--------|--------|--------|--------|--------|--------|--------|--------|--------|--------|
| 0:05 | 642.34 | 640.12 | 638.63 | 638.35 | 637.16 | 636.24 | 635.65 | 635.20 | 634.34 | 633.75 |
| 0:10 | 642.34 | 640.12 | 638.63 | 638.35 | 637.16 | 636.24 | 635.65 | 635.20 | 634.34 | 633.75 |
| 0:15 | 642.31 | 640.12 | 638.63 | 638.35 | 637.16 | 636.24 | 635.65 | 635.20 | 634.34 | 633.75 |
| 0:20 | 642.28 | 640.11 | 638.62 | 638.35 | 637.16 | 636.24 | 635.65 | 635.20 | 634.34 | 633.75 |
| 0:25 | 642.25 | 640.10 | 638.60 | 638.33 | 637.15 | 636.24 | 635.65 | 635.20 | 634.34 | 633.75 |
| 0:30 | 642.23 | 640.09 | 638.58 | 638.32 | 637.14 | 636.23 | 635.64 | 635.19 | 634.34 | 633.75 |
| 0:35 | 642.19 | 640.08 | 638.56 | 638.30 | 637.12 | 636.22 | 635.63 | 635.19 | 634.34 | 633.75 |
| 0:40 | 642.11 | 640.06 | 638.54 | 638.29 | 637.10 | 636.21 | 635.62 | 635.17 | 634.33 | 633.75 |
| 0:45 | 642.06 | 640.04 | 638.50 | 638.26 | 637.08 | 636.19 | 635.60 | 635.16 | 634.33 | 633.74 |
| 0:50 | 642.02 | 640.02 | 638.46 | 638.22 | 637.04 | 636.17 | 635.58 | 635.14 | 634.32 | 633.74 |
| 0:55 | 641.99 | 640.01 | 638.43 | 638.20 | 637.01 | 636.14 | 635.55 | 635.12 | 634.31 | 633.73 |
| 1:00 | 641.96 | 640.00 | 638.41 | 638.18 | 636.98 | 636.11 | 635.53 | 635.09 | 634.29 | 633.73 |
| 1:05 | 641.92 | 639.99 | 638.38 | 638.16 | 636.95 | 636.09 | 635.50 | 635.06 | 634.28 | 633.72 |
| 1:10 | 641.82 | 639.97 | 638.36 | 638.14 | 636.92 | 636.07 | 635.47 | 635.04 | 634.26 | 633.71 |
| 1:15 | 641.76 | 639.94 | 638.32 | 638.11 | 636.90 | 636.05 | 635.45 | 635.01 | 634.25 | 633.70 |
| 1:20 | 641.72 | 639.92 | 638.27 | 638.07 | 636.86 | 636.03 | 635.43 | 634.99 | 634.23 | 633.69 |
| 1:25 | 641.68 | 639.91 | 638.23 | 638.04 | 636.82 | 635.99 | 635.40 | 634.96 | 634.22 | 633.68 |
| 1:30 | 641.63 | 639.89 | 638.20 | 638.02 | 636.78 | 635.96 | 635.37 | 634.93 | 634.20 | 633.67 |
| 1:35 | 641.59 | 639.87 | 638.17 | 638.00 | 636.75 | 635.93 | 635.33 | 634.89 | 634.18 | 633.67 |
| 1:40 | 641.46 | 639.85 | 638.14 | 637.98 | 636.72 | 635.91 | 635.30 | 634.86 | 634.16 | 633.66 |
| 1:45 | 641.38 | 639.80 | 638.09 | 637.95 | 636.69 | 635.89 | 635.28 | 634.83 | 634.14 | 633.64 |
| 1:50 | 641.33 | 639.77 | 638.03 | 637.90 | 636.65 | 635.86 | 635.25 | 634.80 | 634.12 | 633.63 |
| 1:55 | 641.28 | 639.75 | 637.99 | 637.86 | 636.60 | 635.83 | 635.22 | 634.77 | 634.11 | 633.62 |
| 2:00 | 641.22 | 639.72 | 637.95 | 637.83 | 636.56 | 635.79 | 635.18 | 634.73 | 634.09 | 633.61 |
| 2:05 | 641.16 | 639.70 | 637.91 | 637.81 | 636.52 | 635.76 | 635.14 | 634.69 | 634.07 | 633.60 |
| 2:10 | 640.99 | 639.66 | 637.88 | 637.78 | 636.49 | 635.73 | 635.11 | 634.65 | 634.05 | 633.59 |
| 2:15 | 640.91 | 639.60 | 637.83 | 637.75 | 636.46 | 635.70 | 635.08 | 634.61 | 634.02 | 633.58 |
| 2:20 | 640.91 | 639.54 | 637.77 | 637.71 | 636.42 | 635.68 | 635.05 | 634.57 | 634.00 | 633.57 |
| 2:25 | 640.91 | 639.52 | 637.72 | 637.67 | 636.38 | 635.65 | 635.02 | 634.54 | 633.98 | 633.55 |
| 2:30 | 640.91 | 639.51 | 637.69 | 637.63 | 636.34 | 635.62 | 634.99 | 634.50 | 633.96 | 633.54 |
| 2:35 | 640.91 | 639.51 | 637.67 | 637.61 | 636.30 | 635.59 | 634.95 | 634.47 | 633.94 | 633.53 |
| 2:40 | 640.91 | 639.50 | 637.65 | 637.60 | 636.27 | 635.56 | 634.92 | 634.43 | 633.92 | 633.52 |
| 2:45 | 640.91 | 639.50 | 637.65 | 637.59 | 636.25 | 635.54 | 634.89 | 634.39 | 633.90 | 633.51 |
| 2:50 | 640.91 | 639.50 | 637.64 | 637.59 | 636.24 | 635.52 | 634.87 | 634.36 | 633.88 | 633.50 |
| 2:55 | 640.91 | 639.50 | 637.64 | 637.59 | 636.23 | 635.51 | 634.85 | 634.33 | 633.86 | 633.49 |
| 3:00 | 640.91 | 639.50 | 637.64 | 637.59 | 636.23 | 635.50 | 634.83 | 634.30 | 633.85 | 633.47 |
| 3:05 | 640.91 | 639.50 | 637.64 | 637.59 | 636.23 | 635.49 | 634.83 | 634.28 | 633.83 | 633.46 |
| 3:10 | 640.91 | 639.50 | 637.64 | 637.58 | 636.23 | 635.49 | 634.82 | 634.26 | 633.82 | 633.45 |
| 3:15 | 640.91 | 639.50 | 637.64 | 637.58 | 636.22 | 635.49 | 634.82 | 634.25 | 633.81 | 633.44 |
| 3:20 | 640.91 | 639.50 | 637.64 | 637.58 | 636.22 | 635.49 | 634.81 | 634.24 | 633.80 | 633.43 |
| 3:25 | 640.91 | 639.50 | 637.64 | 637.58 | 636.22 | 635.49 | 634.81 | 634.23 | 633.79 | 633.42 |
| 3:30 | 640.91 | 639.50 | 637.64 | 637.58 | 636.22 | 635.48 | 634.81 | 634.22 | 633.79 | 633.42 |
| 3:35 | 640.91 | 639.50 | 637.64 | 637.58 | 636.22 | 635.48 | 634.81 | 634.22 | 633.78 | 633.41 |
| 3:40 | 640.91 | 639.50 | 637.64 | 637.58 | 636.22 | 635.48 | 634.81 | 634.21 | 633.78 | 633.40 |
| 3:45 | 640.91 | 639.50 | 637.64 | 637.58 | 636.22 | 635.48 | 634.81 | 634.21 | 633.78 | 633.40 |
| 3:50 | 640.91 | 639.50 | 637.64 | 637.58 | 636.22 | 635.48 | 634.81 | 634.21 | 633.78 | 633.40 |
| 3:55 | 640.91 | 639.50 | 637.64 | 637.58 | 636.22 | 635.48 | 634.81 | 634.21 | 633.77 | 633.40 |
| 4:00 | 640.91 | 639.50 | 637.64 | 637.58 | 636.22 | 635.48 | 634.81 | 634.21 | 633.77 | 633.39 |
| 4:05 | 640.91 | 639.50 | 637.64 | 637.58 | 636.22 | 635.48 | 634.81 | 634.21 | 633.77 | 633.39 |
| 4:10 | 640.91 | 639.50 | 637.64 | 637.58 | 636.22 | 635.48 | 634.81 | 634.21 | 633.77 | 633.39 |
| 4:15 | 640.91 | 639.50 | 637.64 | 637.58 | 636.22 | 635.48 | 634.81 | 634.21 | 633.77 | 633.39 |
| 4:20 | 640.91 | 639.50 | 637.64 | 637.58 | 636.22 | 635.48 | 634.81 | 634.21 | 633.77 | 633.39 |
| 4:25 | 640.91 | 639.50 | 637.64 | 637.58 | 636.22 | 635.48 | 634.81 | 634.21 | 633.77 | 633.39 |
| 4:30 | 640.91 | 639.50 | 637.64 | 637.58 | 636.22 | 635.48 | 634.81 | 634.21 | 633.77 | 633.39 |
| 4:35 | 640.91 | 639.50 | 637.64 | 637.58 | 636.22 | 635.48 | 634.81 | 634.21 | 633.77 | 633.39 |
| 4:40 | 640.91 | 639.50 | 637.64 | 637.58 | 636.22 | 635.48 | 634.81 | 634.21 | 633.77 | 633.39 |

Results show that the wave critical time depending on distance to the outlet can be approximated to a polynomial trendline with an R^2 equal to 0.9818 (Figure E1, Appendix E Dewatering maps). We use this distribution to create a relation between the distance and the time in which the wave is produced for the different scenarios.

Dewatering speed

It appears clearly that the investigated Storåne river experiences a very rapid dewatering process under the current scenarios produced in 5 minutes. For example, Figure 8 shows the dewatering rate for the scenario A10: in such configuration the whole stream shows dewatering rates over 20 cm/h. Notice that the occidental channel of Ellingøyne and the northern channel in Gjerdeøyne will be completely dried-out at high velocity rate. The same occurs for scenarios A21 & A32 as can be seen in Appendix E. The areas where fish stranding has been observed (Stickler, 2018) are also marked at the maps.

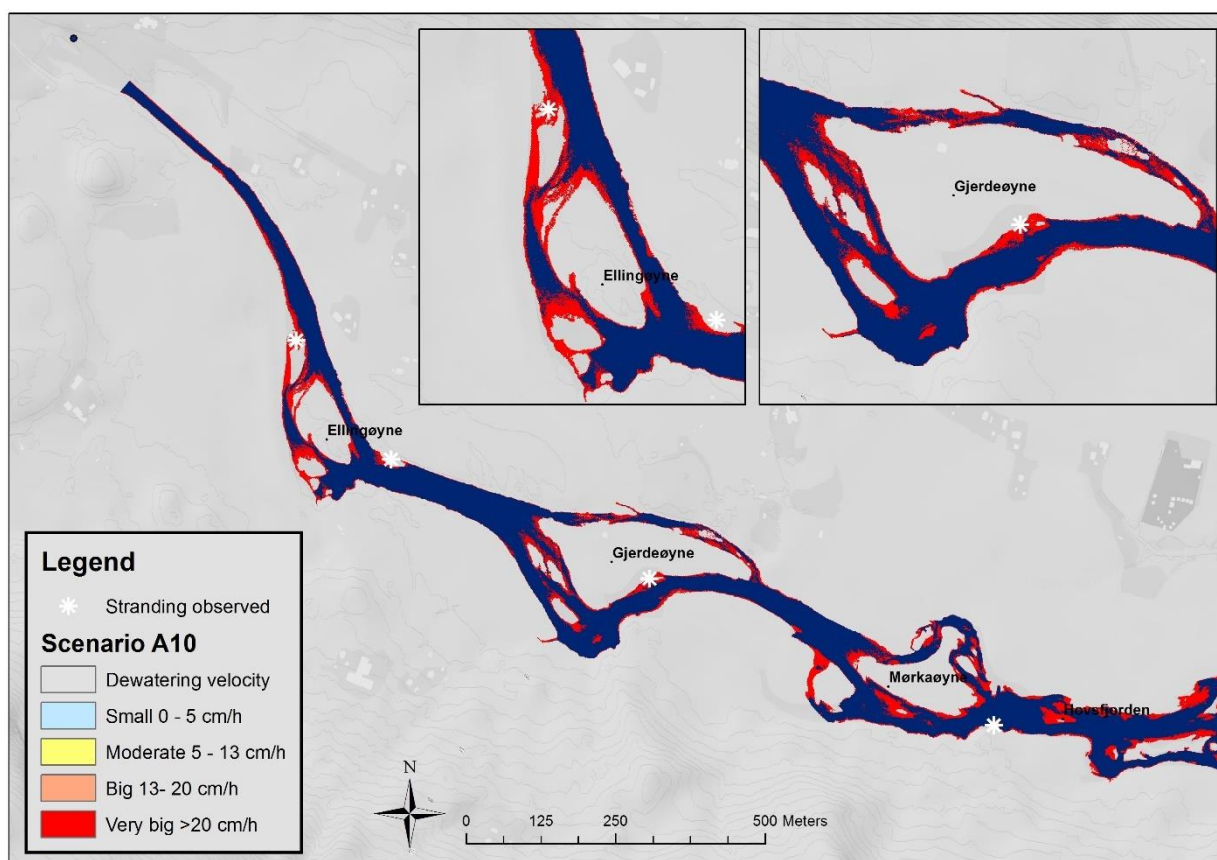


Figure 8. Dewatering rate (cm/h) in scenario A10, blue shows the wetted areas at minimum flow, the rest of colors display the impact in the areas that are dried out, the white stars show the areas where fish stranding has been observed.

6 different dewatering scenarios were tested changing the time of dewatering: 5 min, 10 min, 15 min, 20 min, 25 min and 30 min. The result shows that for 25 min and 30 min the high impact in dewatering only affects the artificial channel but not the natural areas (see appendix F).

The alternative scenarios, B32, B21 & B10, produced in 30 minutes show remarkable improvements in the dewatering rate impact. For scenario B10 (from 21 m³/s to 6m³/s) the dewatering impact in Ellingøyne changes from very big to big and moderate; the dewatering impact around Gjerdeøyne changes from very big to moderate and around Mørkeøyne changes from very big to moderate and small. Notice that the further we are from the outlet the lower the dewatering impact is due to the damping effect (Figure 9).

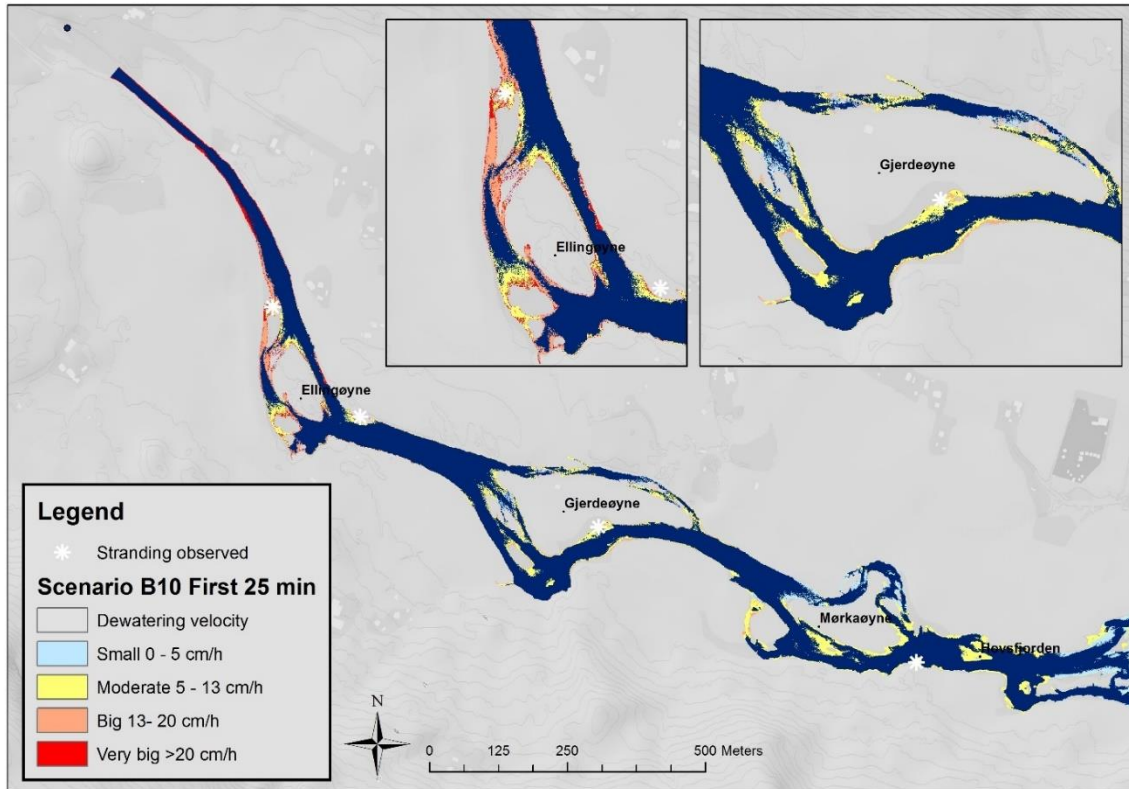


Figure 9. Dewatering rate (cm/h) in scenario B10 in the first 25 min, blue shows the wetted areas at 12 m³/s, the rest of colors display the impact in the areas that are dried out, the white stars show the areas where fish stranding has been observed.

In the alternative scenario we also must consider the last 5 minutes in which turbines are shut down from 40% capacity to no production, due to manufacturer regulations. This situation will also create a steep dewatering wave with big impact (Figure 10) that cannot be avoided by production configurations.

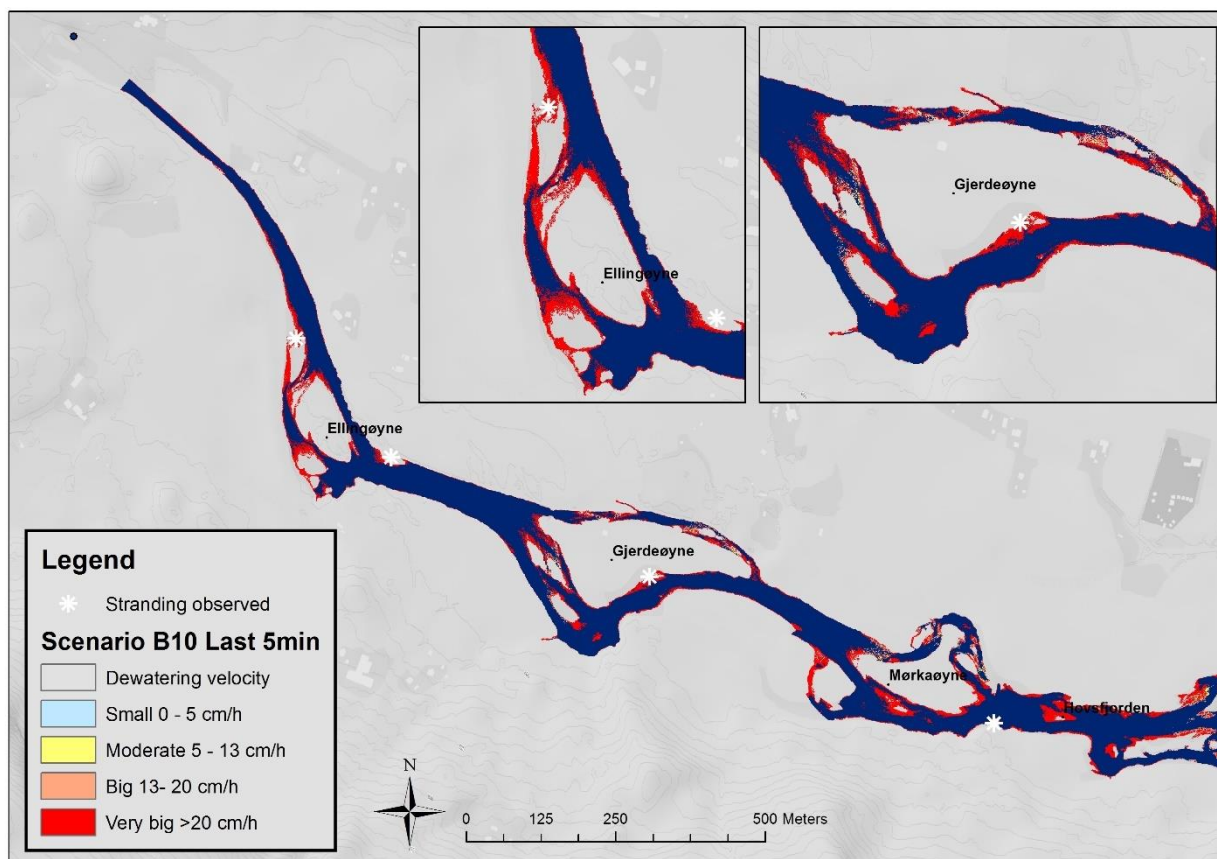


Figure 10 . Dewatering rate (cm/h) in scenario B10 in the last 5 min, blue shows the wetted areas at 12 m³/s, the rest of colors display the impact in the areas that are dried out, the white stars show the areas where fish stranding has been observed.

4. Discussion

The results show that the combination of COSH-Tool to analyze the flow fluctuations, HEC-RAS and GIS processing tools are potential resources to assess the environmental impact in rivers for hydropeaking power plants.

The analysis of the time series in Storåne showed that there are over 300 rapid decreases during the year following the pattern of other hydropeaking rivers (Harby, Alfredsen, Fjeldstad, & Halleraker, 2001). 25% of the rapid decreases end at flows below 18.72 m³/s and 10% below 8.74 m³/s, therefore it is important to analyze the dried-out areas and dewatering rates for low flows to assess the stranding impact in brown trout (Halleraker J. H., 2003). The seasonal analysis did not show specific variation during winter, potentially due to the operation restrictions that forbid stopping the power plants during winter due to risk of freezing in the penstock.

The calibration results show that having a high-resolution geomorphology and bathymetry input can overcome the challenge of calibrating the model. The measured mean error from comparison with GPS measures was 6 cm. It is worth noticing that the accuracy of the LiDAR data is 3 cm (Alne, 2016) and for the GPS points measured is between 1.5 and 3 cm. Therefore, we can ensure that the model is well calibrated. For further studies it would be interesting to introduce the fjord water surface elevation as an input boundary condition.

The simulations show that the lower the flow the higher the rate of increase in dried areas. The wetted area is dramatically decreased below 21 m³/s and specially below 12m³/s. The western stream in Ellingøyne and northern stream in Gjerdeøyne will completely disappear in this range. Below 6 cm water depth we enter the uncertainty range of the model, therefore we cannot ensure whether the area will be dried or wet when depth is between 0 and 6 cm.

Simulations show that the damping effect is a key factor to evaluate the dewatering rate. The wave that is produced in 5 minutes in the outlet will be attenuated reaching one hour and a half at the end of the study site.

This study shows that a change in the operation can improve stream conditions, reducing stranding risk for brown trout. The current scenarios that the company operates the power plant (A10, A21 & A32) show a very big impact in the dewatering rate for all the range of flows. The alternative suggested scenarios (B10, B21 & B32) reduce the impact to moderate and small according to the Handbook for Environmental Design in Regulated Salmon (Bakken, Forseth, & Harby, 2016). The alternative, changing the scenario duration from 5 min to 30 min showed to be the most appropriate according to the dewatering rates. The maps show that the dewatering rates in natural areas are below 20 cm/h in the reach when the duration is 25 minutes or higher. As mentioned before, there is a special high impact when flow is below 21 m³/s, therefore the first step to reduce impact by operational measures would be changing the shut down time when flow is below this value, meaning that when there is only one turbine working this should be shut down following the scenario B10. It is important to mention that even if we change the operation time, due to turbines limitation there will be a high impact wave for the last 40% of the capacity. Furthermore, if we impose a delayed shut down 300 hundred days per year it would have a cost, estimated as 1.5 mill.NOK/year (Appendix J).

Even if this analysis shows a high impact for the dried areas and dewatering speed, the impacts on the riverine ecosystem can only be assessed in combination with biological data (e.g. fish spawning locations, diversity in invertebrate species) and further abiotic data (e.g. substrate, water temperature). Substrate is generally very important for brown trout. It can be used as shelter from predators using interstitial spaces (Heggenes, 1988; Heggenes, Bagliniere, & Cunjak, 1999). According to Bachman, 1984, coarser over finer substrates are important for brown trout. We find this distribution in the area surrounding Ellingøyne and the northern stream of Gjerdeøyne (Appendix F), both with a substrate distribution of more than 45 % over 10 cm and low percentage of fines less than 5% (Appendix G). Therefore, we think they would be potential areas to implement habitat measures (Appendix F).

It is also worth to mention that Salveit & Braband, 2016 carried out an study of fish density in 8 stations in Storåne (Appendix H). Three were located upstream the outlet and five downstream the outlet of Hol I. The fish density downstream the outlet was shown to be clearly lower than upstream. This fact may be a consequence of the substrate in which these measurements took place but also the hydropower operation.

This study has shown to be good methodology thanks to the available LiDAR data and the development of new 2D-model software that replaced one-dimensional hydraulic models that aim to analyze fish stranding by creating several cross sections (Casas-Mulet, Alfredsen, Boissy, & Rütther, 2014). It could easily be applied in other streams where appropriate geomorphological data is accessible, for example in the outlet of Hemsil II hydropower plant, where a similar procedure is planned to be carried out. This station is also located in Hallingdal in the municipality of Gol and LiDAR scan is already available. In Appendix H results from a trial simulation with $Q=30$ m³/s are shown.

Acknowledgements: A first version of this article is presented as a Master Thesis in NTNU in June 2018. The author thanks E-CO Energi, especially Bjørn Otto Dønnum for providing all the data. Also, thanks to Morten Stickler for insights in the river environment and presenting data, and to Marcin for helping in processing the ADCP measurements.

References

- Adeva Bustos, A., Hedger, R. D., Fjeldstad, H.-P., Alfredsen, K., Sundt, H., & Barton, D. N. (2017). Modeling the effects of alternative mitigation measures on Atlantic salmon production in a regulated river. *Elsevier*, 32-41.
- Ahonen, J. (2018). *Can morphologic restoration of hydropower outlet channels create hydraulically suitable spawning and larvae habitats for grayling?* UMEÅ Universitet. Digitala Vetenskapliga Arkivet.

- Ahonen, J. (2018). *Can morphologic restoration of hydropower outlet channels create hydraulically suitable spawning and larvae habitats for grayling? : Modelling the effects of environmental measures with HEC-RAS*. Hentet 6 12, 2018 fra <http://umu.diva-portal.org/smash/record.jsf?pid=diva2:1177275>
- Alne, I. S. (2016). *Topo-Bathymetric LiDAR for Hydraulic Modeling*. Trondheim: NTNU.
- Bachman, R. A. (1984). Foraging behaviour of free-ranging wild and hatchery brown trout in a stream. *Trans. Am. Fish. Soc.*, 1-32.
- Bakken, H., Forseth, T., & Harby, A. (2016). *Handbook for Environmental Design in Regulated Salmon Rivers*. Trondheim: NINA Temahefte 62.
- Bendiksby, L. (2013). *Fiskeundersøkelser i forbindelse med revisjon av Holsreguleringen*. Oslo: Tech. rep. Norconsult AS.
- Bradford, M. J. (1998). An experimental study of stranding of juvenile salmonids on gravel bars and in side channels during rapid flow decreases. *Regulated rivers: Research & Management*, 395-401.
- Casas-Mulet, R., Alfredsen, K., Boissy, T., & Rüther, N. (2014). Performance of a one-dimensional hydraulic model for the calculation of stranding areas in hydropeaking rivers. *Wiley Online Library*, 143-155.
- Center, H. E. (2018, Jun 7). *US Army Corps*. Hentet fra Hec-ras: <http://www.hec.usace.army.mil/software/hec-ras/>
- Choi, S.-U., Kim, S. K., Choi, B., & Kim, Y. (2017). Impact of hydropeaking on downstream fish habitat at the Goesan Dam in Korea. *Ecohydrology*, 10, 10.1002/eco.1861.
- Csanyi May, N., & Toth, C. K. (2007). Point positioning accuracy of airborne LiDAR systems: a rigorous analysis. *International Archives of Photogrammetry, Remote Sensing and Spatial Information Sciences*, 36, 107-111.
- Cushman, R. M. (1985). Review of ecological effects of rapidly varying flows downstream of hydroelectric facilities. *North American Journal of Fisheries Management*, 330-339.
- Dønnum, B. O. (2016). *Hol I- operation limitations for the different turbines*.
- E-co 100% Ren Energi*. (2018, 05). Hentet fra <http://www.e-co.no/Norsk/Forside/Kraftverk/Hallingdal/>
- European Commission*. (2018, 05 22). Hentet fra Climate Action: https://ec.europa.eu/clima/policies/strategies/2050_en
- Flodmark, L. E., Vøllestad, L. A., & Forseth, T. (2004). Performance of juvenile brown trout exposed to fluctuating water level and temperature. *Journal of Fish and Biology*, 460-470.
- G. Berland, T. N. (2004). Movements of wild Atlantic salmon parr in relation to peaking flows below a hydropower station. *River research and Applications*, 957-966.
- Georg Premstaller, V. C. (2016). Hydropeaking mitigation project on a multi-purpose hydro-scheme on Valsura River in South Tyrol/Italy. *Science of the Total Environment*, 12.

- Gostner, W., Lucarelli, C., Theiner, D., Krager, A. P., & Schleiss, A. (2011). A holistic approach to reduce negative impacts of hydropeaking. *Dams Reserv. under Chang. Challenges*, 857-865.
- Halleraker J. H., S. S. (2003). Factors influencing stranding of wild juvenile brown trout (*Salmo Trutta*) during rapid and frequent flow decreases in an artificial stream. *Wiley InerScience*, 15. Hentet fra <https://onlinelibrary.wiley.com/doi/epdf/10.1002/rra.752>
- Harby, A., Alfredsen, K. T., Fjeldstad, H. P., & Halleraker, J. H. (2001). Ecological impacts of hydro peaking in rivers. *International Conference on Hydropower Development*. Lisse, Netherlands: Balkema.
- Hauer, C., Holzapfel, P., Leitner, P., & Graf, W. (2016). Longitudinal assessment of hydropeaking impacts on various scales for an improved process understanding and the design of mitigation measures. *Science of the Total Environment*, 1503-1514.
- Heggenes, J. (1988). Effects of short-term flow fluctuations on displacement of, and habitat use by, brown trout in a small stream. *Trans. Am. Fish. Soc.*, 336-344.
- Heggenes, J., Bagliniere, J. L., & Cunjak, R. A. (1999). Spatial niche variability for young Atlantic salmon and brown trout in heterogeneous streams. *Ecol. Fresh. Fish*, 1-21.
- Ingeborg Graabak, S. J. (2017). Norway as a Battery for the Future European Power System-Impacts on the Hydropower System. *Energies*, 25.
- Julian Friedrich Sauterleute, J. C. (2014). A computational tool for the characterisation of rapid fluctuations in flow and stage in rivers caused by hydropeaking. *Environmental Modelling and Software*, 12.
- Lauters, F., Lavandier, P., Lim, P., & Belaud, A. (1996). Influence of hydropeaking on invertebrates and their relationship with fish feeding habits in a Pyrenean river. *Regulated rivers: Research & Management*, 563-573.
- Monk, S. (2016). Modeling: Using 2D HEC-RAS to Determine Fish Passability and Habitat Quality. *International Convergence on Engineering and Ecohydrology for Fish Passage*. University of Massachusetts.
- Nagrodski, A., Raby, G. D., Hasler, C. T., Taylor, M. K., & Cooke, S. J. (2012). Fish stranding in fresh water systems: Sources, consequences and mitigation. *Journal of Environmental Management*, 133-141.
- NVE. (2018, 05 22). Hentet fra Norges vassdrags- og energidirektorat (NVE): <https://www.nve.no/energiforsyning-og-konsesjon/vannkraft/revisjon-av-konsesjonsvilkar/>
- Person, E. (2013). *Impact of hydropeaking on fish and their habitat*. Hentet fra <http://dx.doi.org/10.5075/epfl-thesis-5812>
- Premstaller, G., Cavedon, V., Pisaturo, G. R., Schweizer, S., Adami, V., & Righetti, M. (2016). Hydropeaking mitigation project on a multi-purpose hydro-scheme on Valsura River in South Tyrol/Italy. *Science of the Total Environment*, 642-654.
- Salveit, S. J., & Braband, Å. (2016). *Tetthet av ørret i Storåne i september 2016*. Nordconsult.

- Salveit, S. J., Halleraker, J. H., Arnekleiv, J. V., & Harby, A. (2001, September). Field experiments on stranding juvenile atlantic salmon (*Salmo salar*) and brown trout (*Salmo trutta*) during rapid flow decreases caused by hydropeaking. *Regulated rivers: Research and management*, 609-622.
- Stickler, M. (2018, 02). Observed stranding areas. (A. Juarez, Intervjuer)
- Stillwater Sciences. (2006). *Flow fluctuations and stranding at the Carmen-Smith Hydroelectric Project, Upper McKenzie River Basin, Oregon*. Oregon: Eugene Water & Electric Board.
- T. Vehanen, P. B.-P. (2000). Effect of fluctuating flow and temperature on cover type selection and behaviour by juvenile brown trout in artificial flumes. *Journal of Fish Biology*, 923-937.
- Tuhtan, J. A., Noack, M., & Wieprecht, S. (2011). Estimating Stranding Risk due to Hydropeaking for Juvenile European Grayling Considering River Morphology. *KSCE Journal of Civil Engineering*, 197-206.
- USACE. (2018, 04 10). Hentet fra HEC-RAS: <http://www.hec.usace.army.mil/software/hec-ras/>
- Vanzo, D., Siviglia, A., Giido, Z., Alfreden, K., & Tancon, M. (2016). A modeling approach for the quantification of fish stranding risk, the case of Lundesokna river. *11th ISE*. Melbourne.
- Vanzo, D., Tancon, M., Zolezzi, G., & Siviglia, A. (2014). A Modeling Approach For The Quantification Of Fish Stranding Risk: The Case Of Lundesokna River (Norway). *11th International Symposium on Ecohydraulics*. Australia.
- Vanzo, D., Tancon, M., Zolezzi, G., Alfredsen, K., & Siviglia, A. (2016). A modeling approach for the qualification of fish stranding risk: the case of Lundesokna river. *ResearchGate*, 8.
- Vanzo, D., Tancon, M., Zolezzi, G., Alfredsen, K., & Siviglia, A. (2016). A Modeling Approach For The Quantification Of Fish Stranding Risk: The Case Of Lundesokna River (Norway). *ResearchGate*, 8.
- Yin, X. A., Yang, Z. F., & Petts, G. E. (2012). Optimizing enviromental flows below dams. *River Res. Appl.* 28, 703-716.

Appendix A COSH Tool extra figures Appendix A COSH Tool extra figures

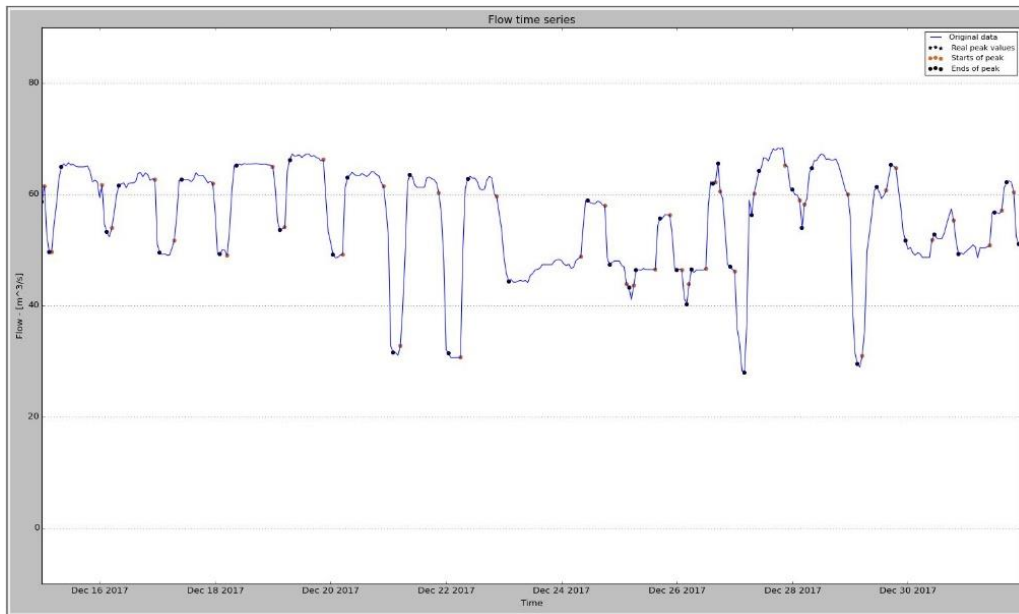


Figure A1. Time series from December 15th to December 31st of 2017 with identified rapid increases and decreases.

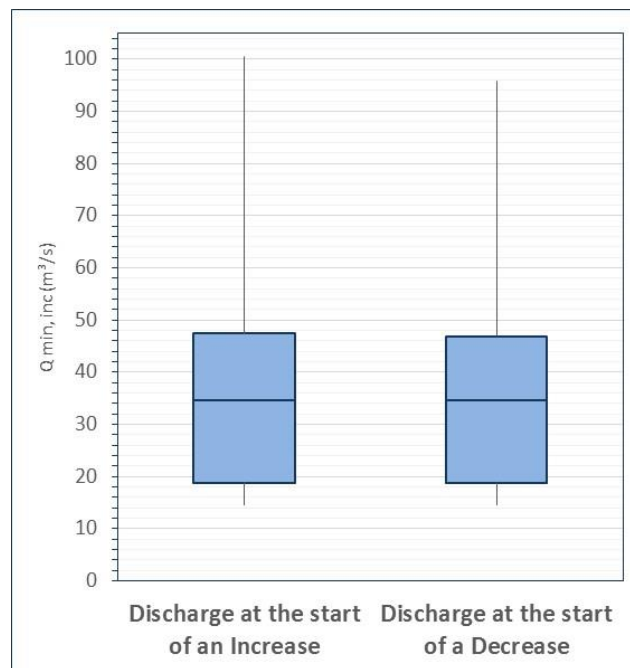


Figure A2. Discharge at the start of an increase (left) and the end of a decrease (right) 2010-2018 downstream Hol I hydropower plant.

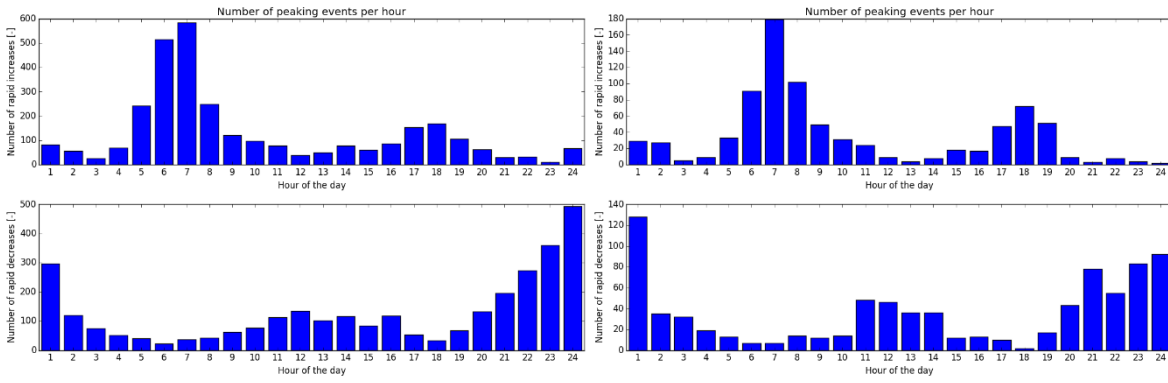


Figure A3. Total number of peaking events per hour in total year (left) and winter season (right) downstream of Hol I hydropower plant.

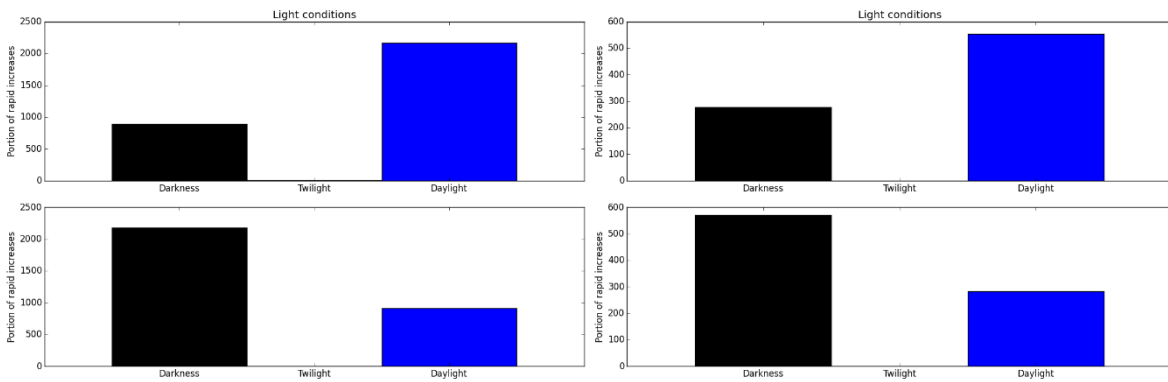


Figure A4. Number of fluctuation during the whole year (left) and winter season (right) during darkness, twilight and daylight downstream of Hol I hydropower plant.

Appendix B Model calibration

| Data source | Discharge (m ³ /s) | Date |
|----------------------------|-------------------------------|--|
| Water edge from ALB survey | 31.72 | October 3 rd , 2015 |
| GPS points | 15.48-44.72 | September 19 th & 20 th , 2016 |
| Norge I Bilder pictures | 2.44 | July 15 th , 2006 13:47 |

Table B1 Summary of calibration resources, the correspondent discharge and date.

B.1 Comparison with Water edge from ALB survey

| Parameter | Value (m ³ /s) |
|--------------------|---------------------------|
| Mean | 31.35 |
| Max | 31.72 |
| Min | 30.11 |
| Standard deviation | 0.41 |

Table B2 Descriptive statistics of the discharge in Storåne on October 3rd between 5:00 and 22:00, the day of the ALB survey

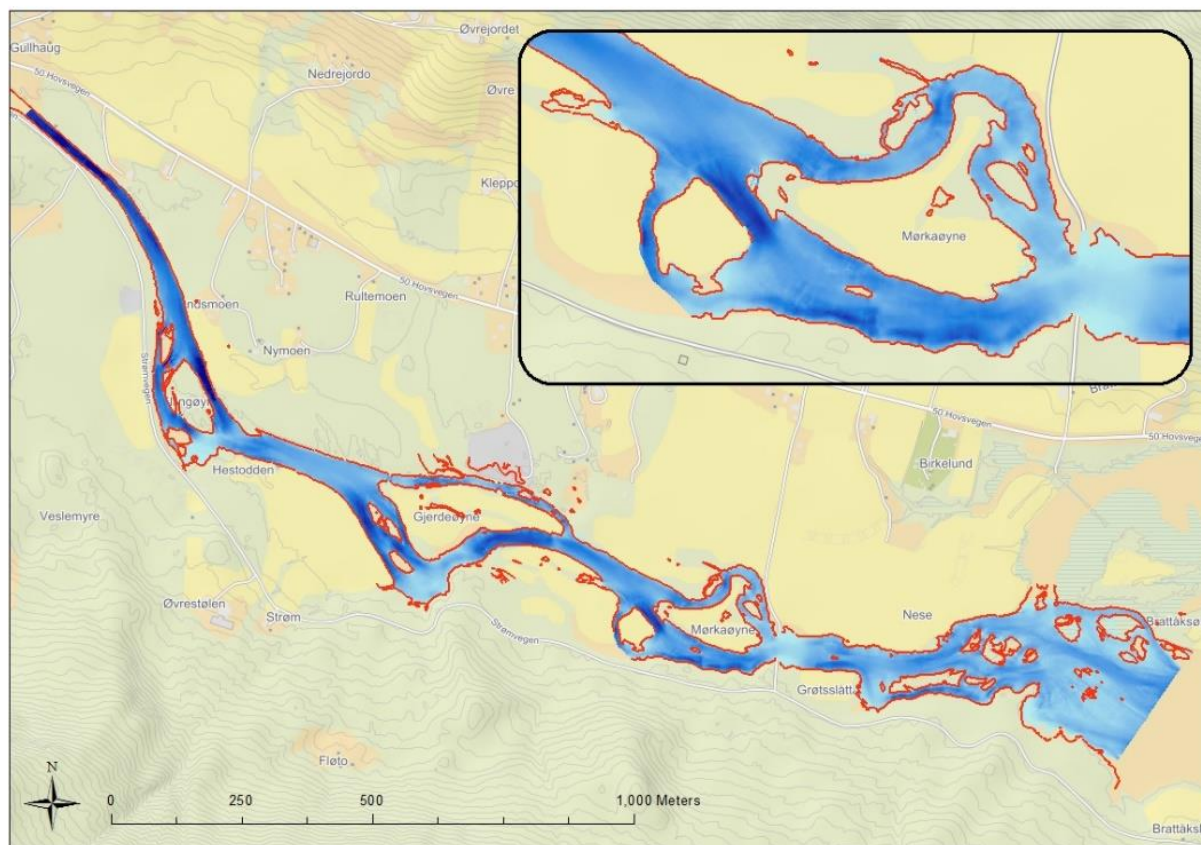


Figure B1 Comparison of model simulation with water edge recorded the day of the flight (Red)

B.2 GPS Measurements

The GPS measurements were taken by Iacopo Muscaral in September 19th and 20th 2016. Data was collected by using a Leica Viva Differential GPS (Picture 3.3) with an accuracy of 0.01-0.02 m in the XY direction and 0.015-0.03 m in the Z direction.

Table B3 GPS points groups depending on discharge measured on the different time intervals.

| Group | Day | Time interval | Discharge (m ³ /s) |
|-------|--------|---------------|-------------------------------|
| A | 19-Sep | 09:00-12:00 | 44.72 |
| B | 19-Sep | 12:00-20:00 | 43.82 |
| C | 20-Sep | 09:00-12:00 | 15.70 |
| D | 20-Sep | 12:00-20:00 | 15.48 |

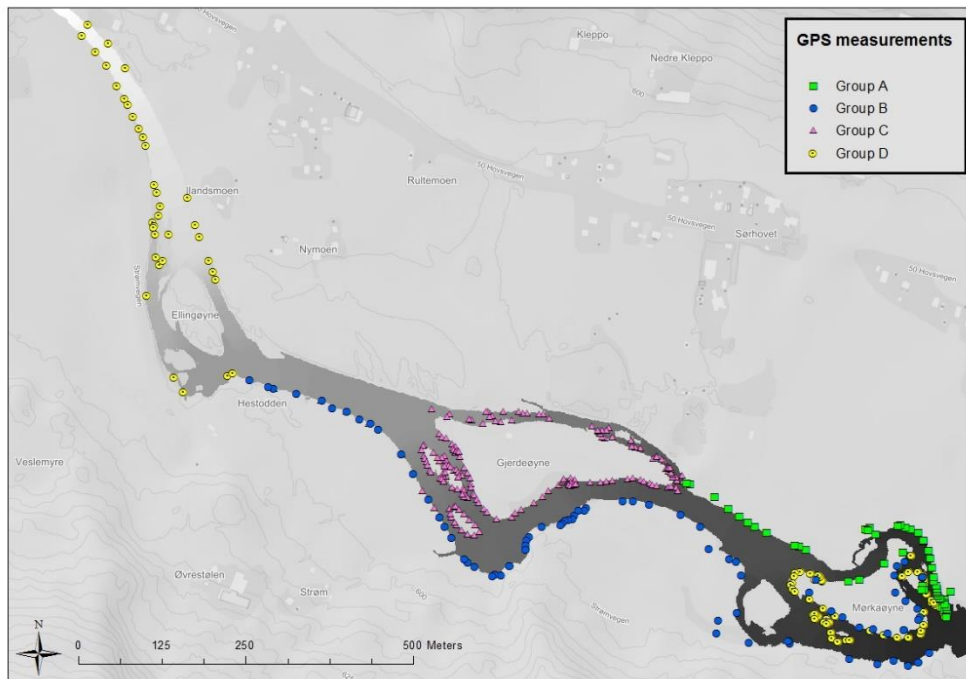


Figure B2 GPS measured point along Storåne divided into 4 different groups depending on the discharge at the different times.

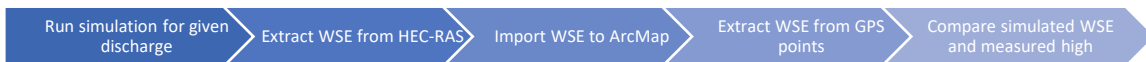


Figure B2 Work flow for model calibration in Storåne

B.3 Low discharge calibration

Low flow calibration was made by comparison with a picture taken in 2006 during a low flow day.

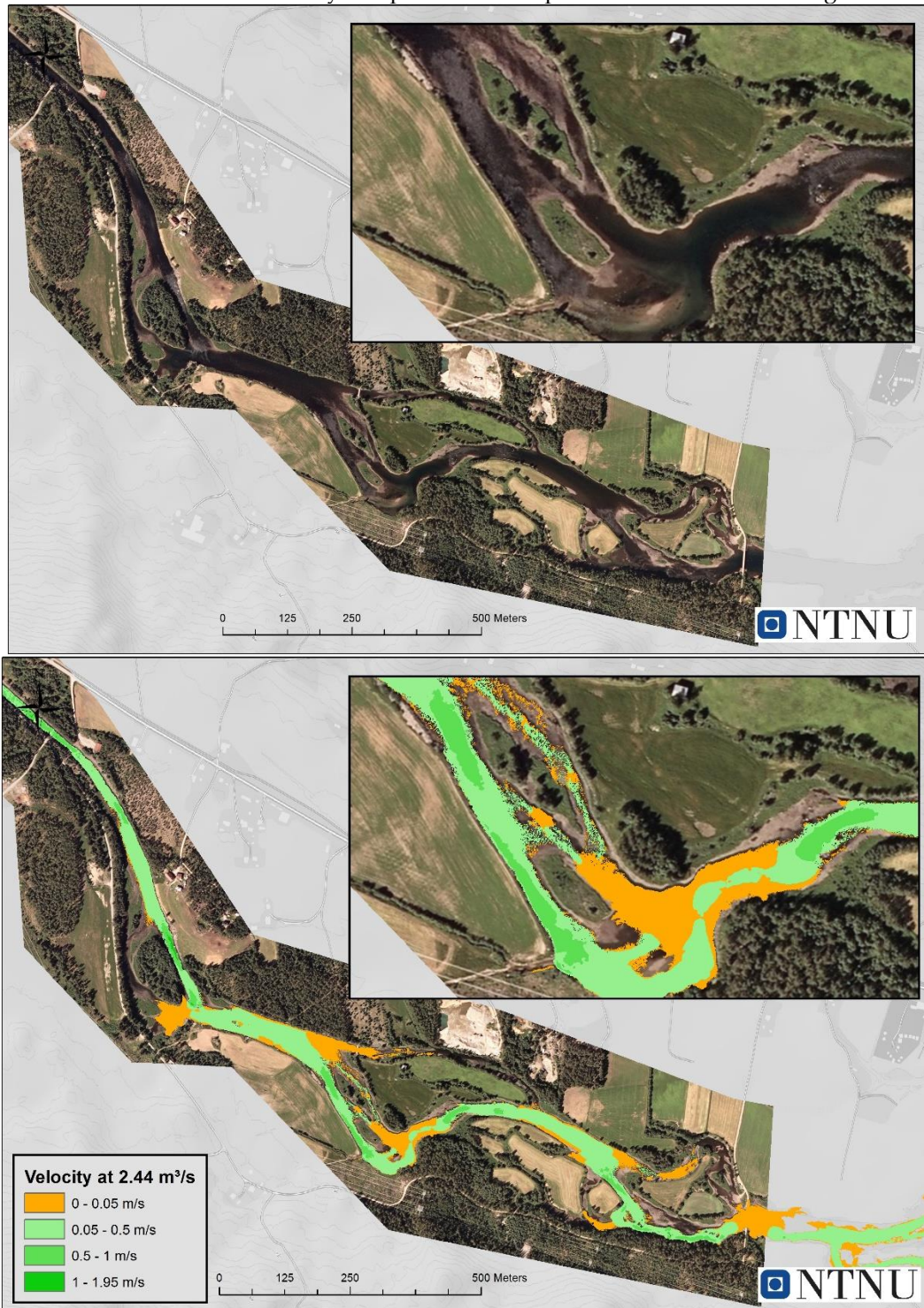


Figure B3 Comparison Norge I Bilder 2.44 m³/s (Top), Norge I Bilder picture with model for 2.44 m³/s overlapped (Bottom)

| Parameter | Discharge (m ³ /s) |
|--------------------|----------------------------------|
| Mean | 2.34 |
| Max | 2.65 |
| Min | 1.97 |
| Standard deviation | 0.17 |

Table B4 Descriptive statistics of flow in Storåne July 15th, 2006 between 5:00 to 22:00 the day of the picture by Norge i Bilder (NVE, database)

B.4 Velocity comparison between model and field measurements

Velocity profiles were taken on May 9th, 2018. In location G located in Gjerdeøyne next to the bridge measures were taken between 13:31 and 13:43. In location M located in Morkeøyne the measures were taken between 17:31 and 17:42. The discharge recorded in this time frame were between 39.98 m³/ & 54.76 m³/s (T

| Day & time | Discharge (m ³ /s) |
|------------------|-------------------------------|
| 2018-05-09 12:00 | 39.98 |
| 2018-05-09 13:00 | 41.37 |
| 2018-05-09 14:00 | 43.59 |
| 2018-05-09 15:00 | 47.10 |
| 2018-05-09 16:00 | 50.95 |
| 2018-05-09 17:00 | 54.76 |

Table B5 Discharge recorded May 9th during velocity profiles measurements.

Results in location G were very similar in model and field measurements while in location M the comparison did not give similar results. A reason probably reason for that is the effect of the water level in Hovsfjorden, that can change the behavior of water in Morkeøyne. For further work it would be interesting to introduce in the model this boundary condition but for that more extensive data would be required.

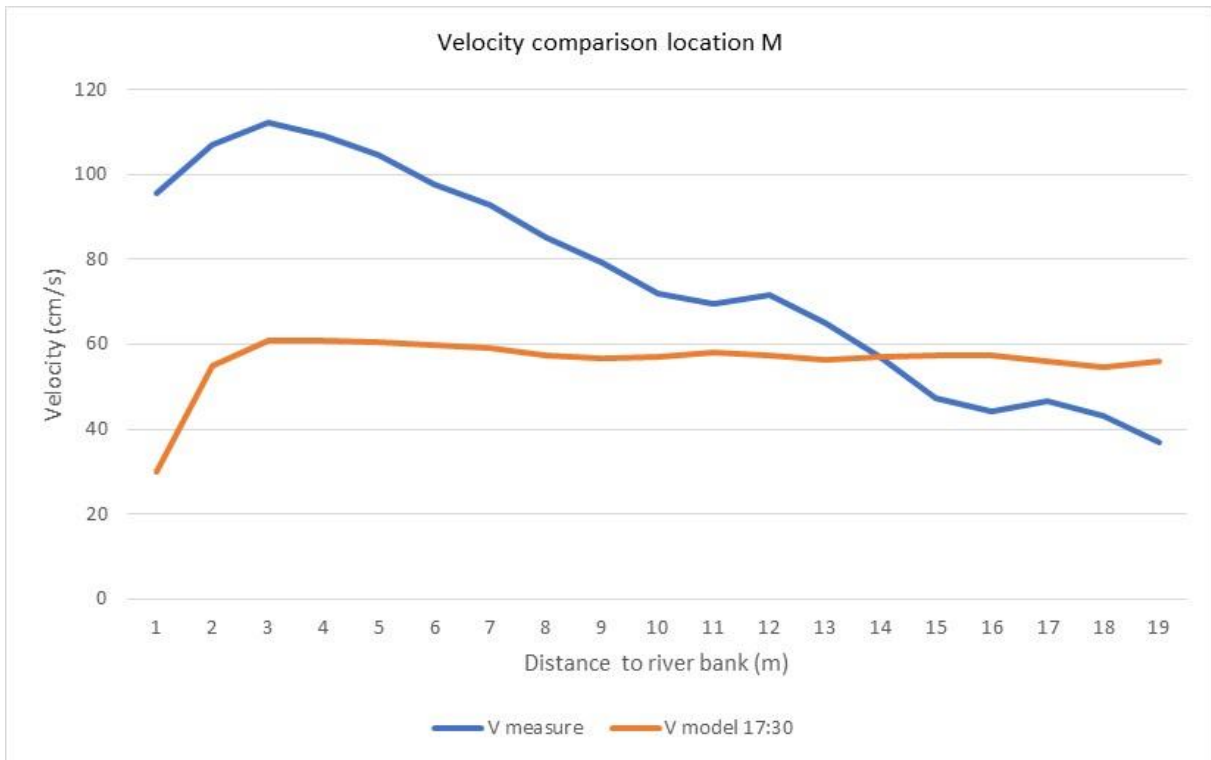


Figure B4 Velocity profile in location M

Appendix C Dried out map for different discharges and velocities

Results show that the lower the flow the more percentage of dried-out area. We represent discharge against dried out area showing a critical point for 12 m³/s (**Figure 1**Figure).

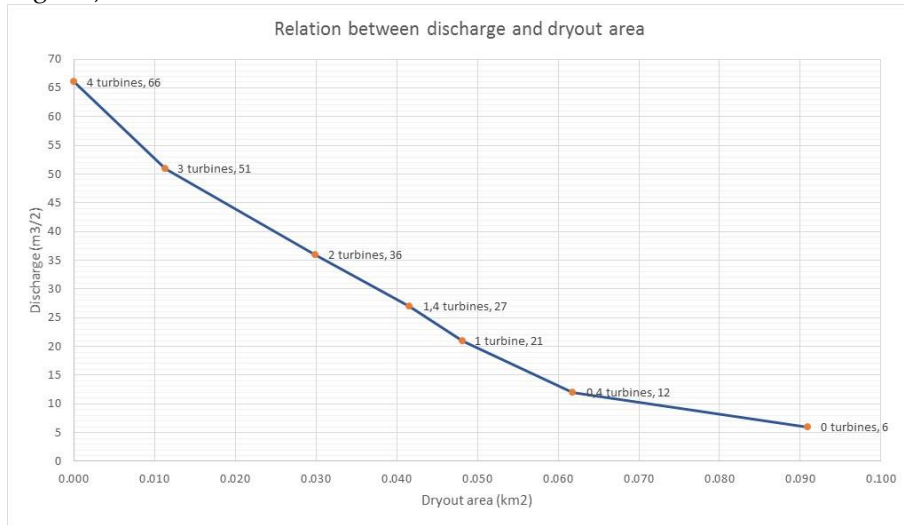


Figure C1 Discharge against dried out area downstream Hol I hydropower plant

We represent in maps the wetted areas depending on different discharges chosen by the different scenarios configuration. Color blue represents the wetted area for minimum flow, red color represents the additional wetted area when one turbine is functioning, orange represent the additional wetted area when 2 turbines are working, correspondingly yellow color is the additional area when 3 turbines are working and finally the green color is also the wetted area when the 4 turbines plus base flow are flowing (66m³/s).

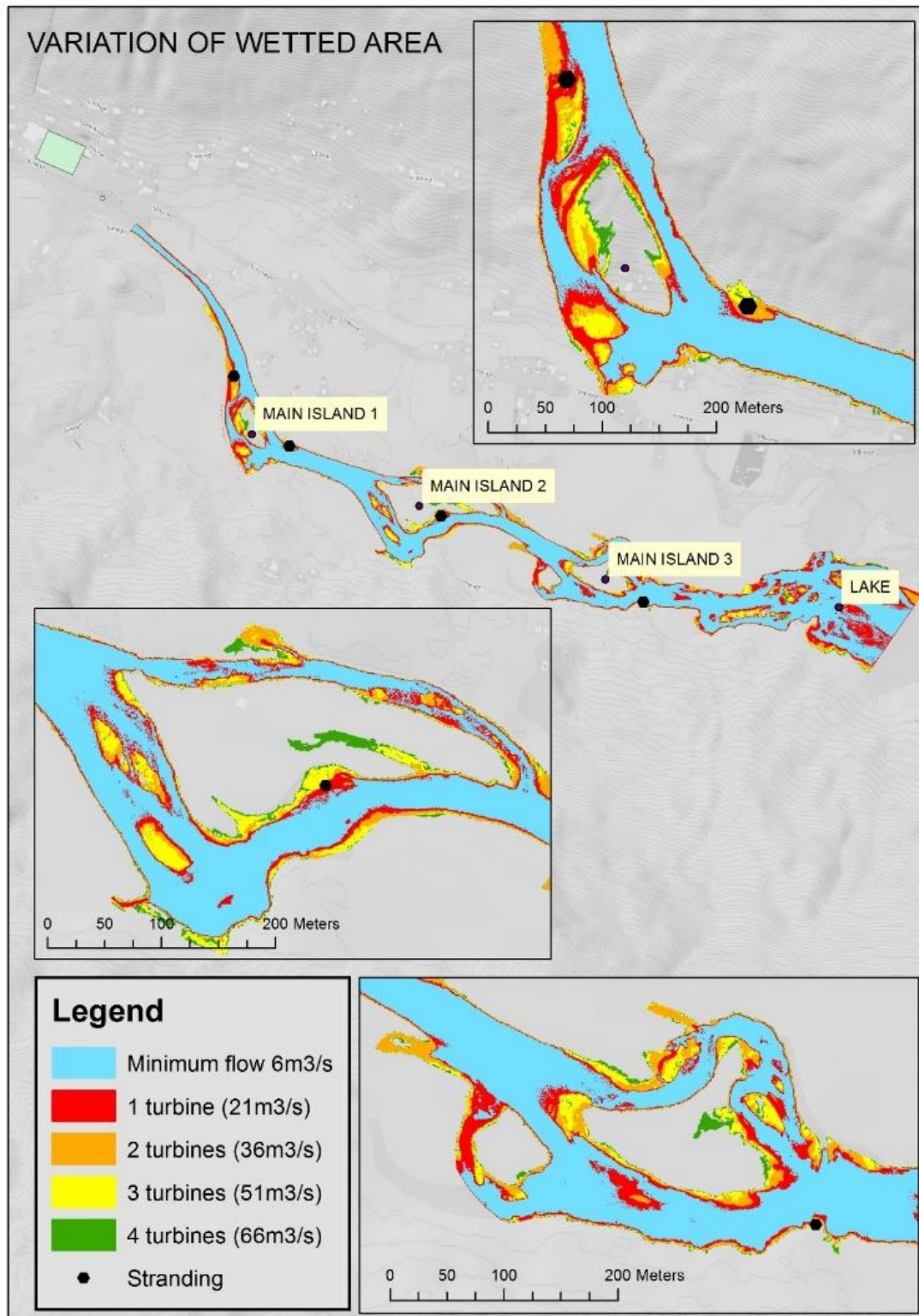


Figure C2 Variation of wetted area: in blue the wetted area at base flow (6m³/s); in red the area dried passing from 1 turbine to base flow (21m³/s); in orange from 2 to 1 turbine (36m³/s); in yellow from 3 to 2 turbines (51m³/s) & in green from 4 to 3 turbines (66m³/s)

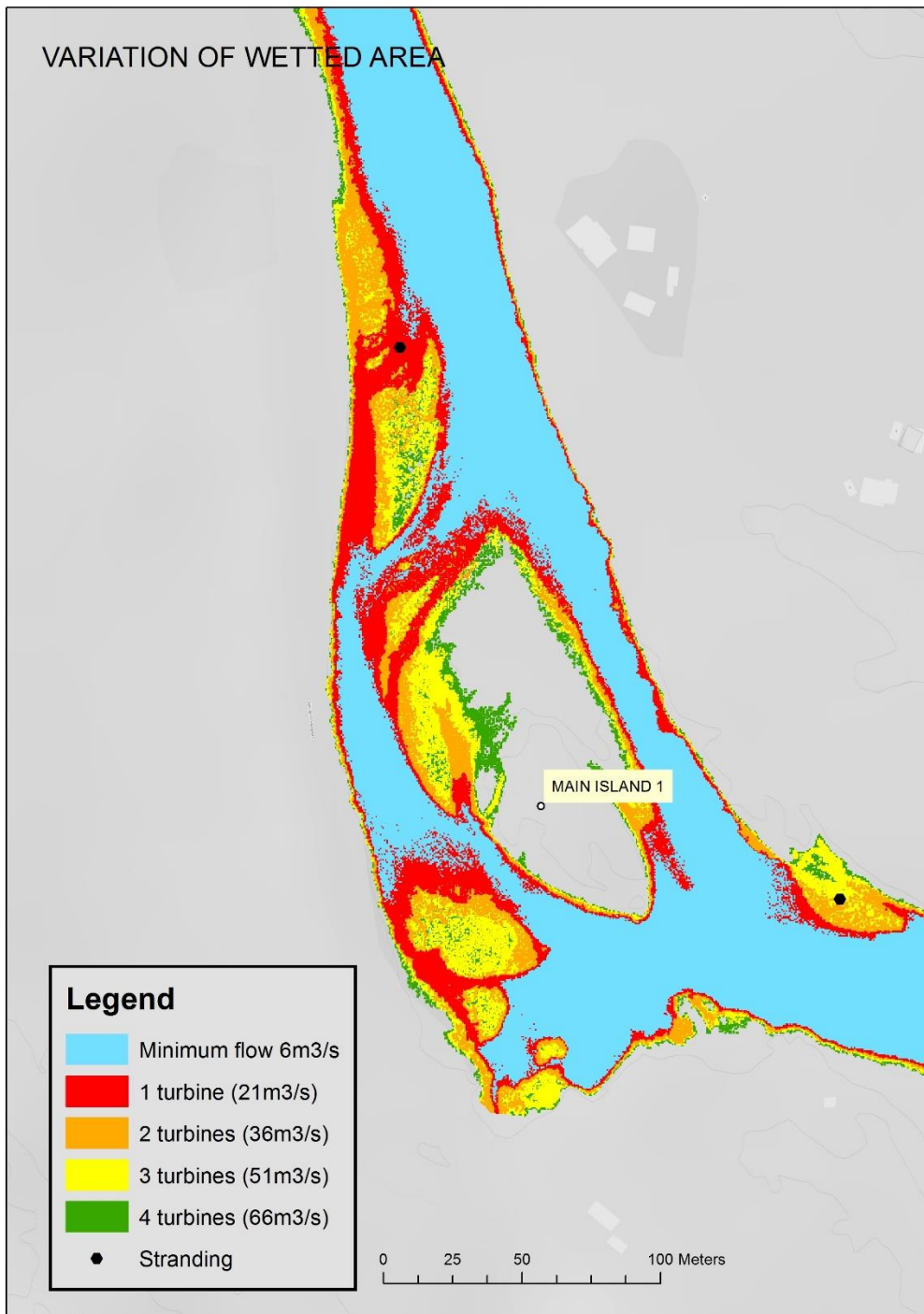


Figure C3. Variation of wetted area in Ellingøyne: in blue the wetted area at base flow (6m³/s); in red the area dried passing from 1 turbine to base flow (21m³/s); in orange from 2 to 1 turbine (36m³/s); in yellow from 3 to 2 turbines (51m³/s) & in green from 4 to 3 turbines (66m³/s)

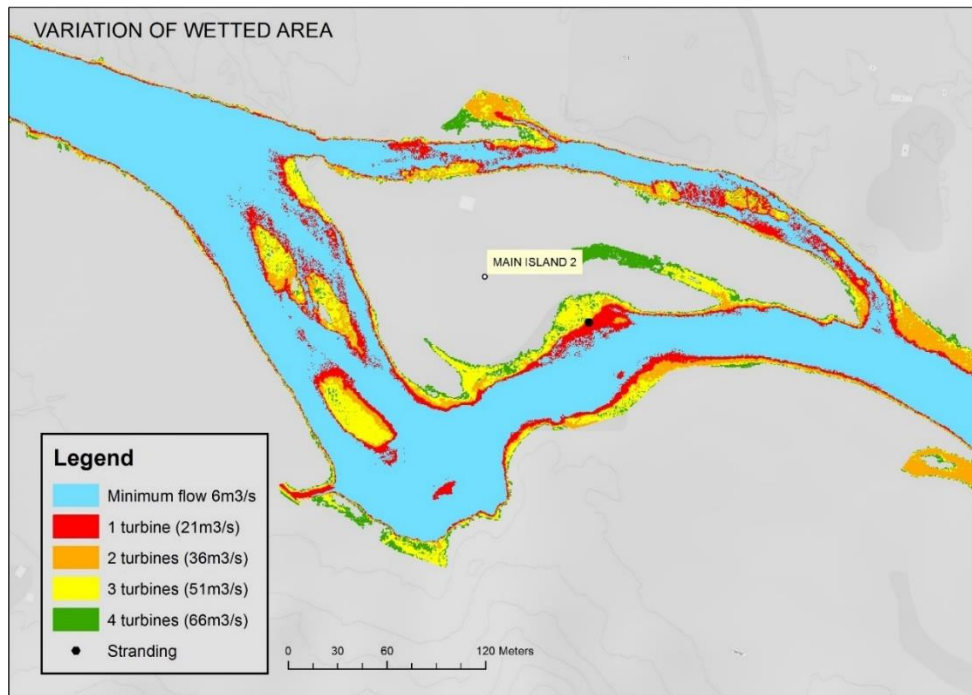


Figure C4. Variation of wetted area in Gjerdeøyne: in blue the wetted area at base flow (6m³/s); in red the area dried passing from 1 turbine to base flow (21m³/s); in orange from 2 to 1 turbine (36m³/s); in yellow from 3 to 2 turbines (51m³/s) & in green from 4 to 3 turbines (66m³/s)

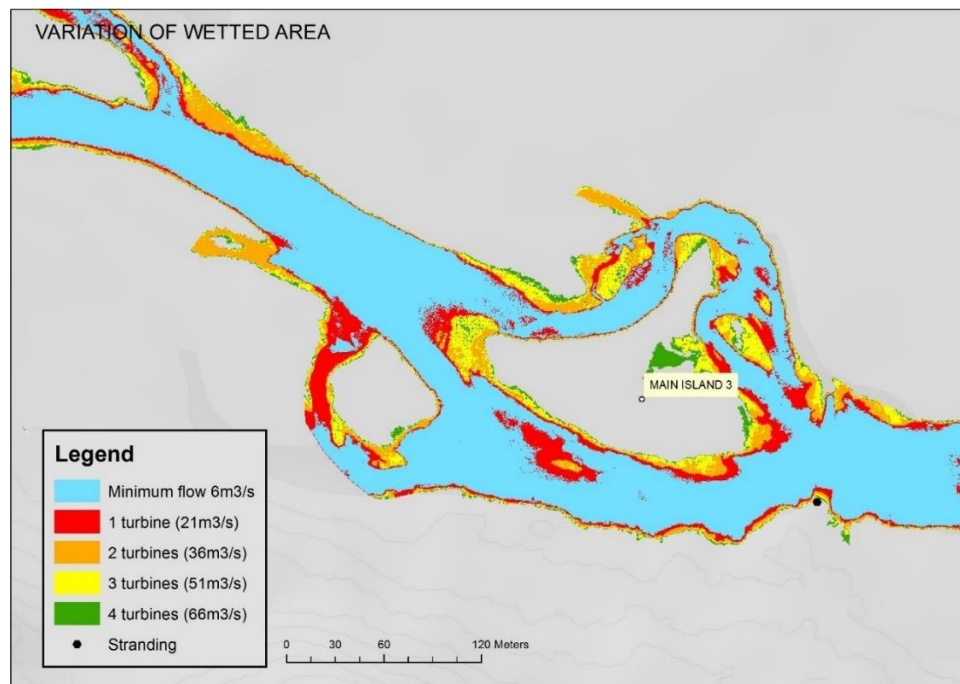


Figure C5. Variation of wetted area in Morkaøyne: in blue the wetted area at base flow (6m³/s); in red the area dried passing from 1 turbine to base flow (21m³/s); in orange from 2 to 1 turbine (36m³/s); in yellow from 3 to 2 turbines (51m³/s) & in green from 4 to 3 turbines (66m³/s)

Appendix D Georeferenced pictures taken with drone in Storåne

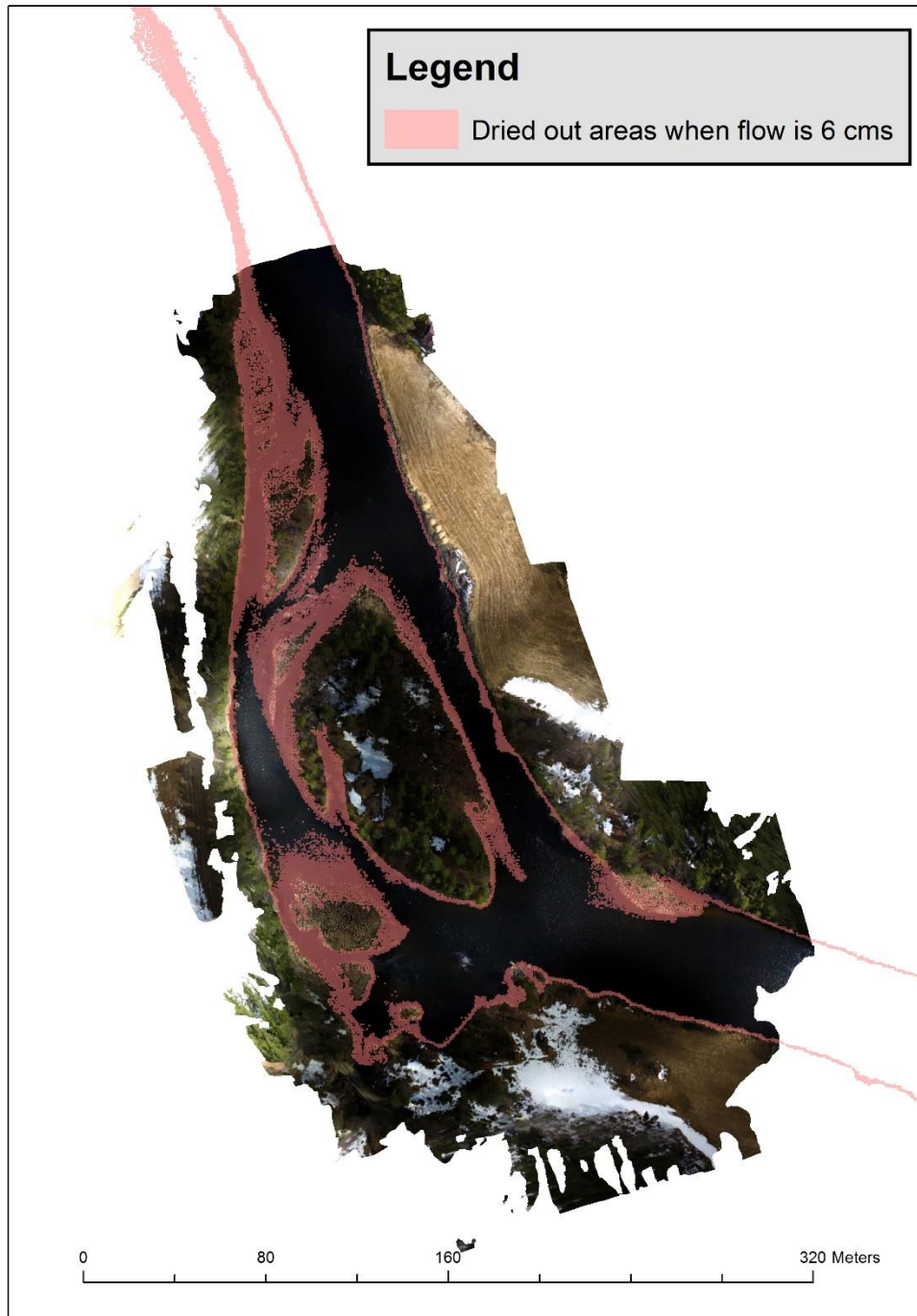


Figure D1. Ellingøyne island in Storåne with the dried-out areas when discharge is $6 \text{ m}^3/\text{s}$. Picture taken with Drone DJI Phantom 3 the May 9th, 2018

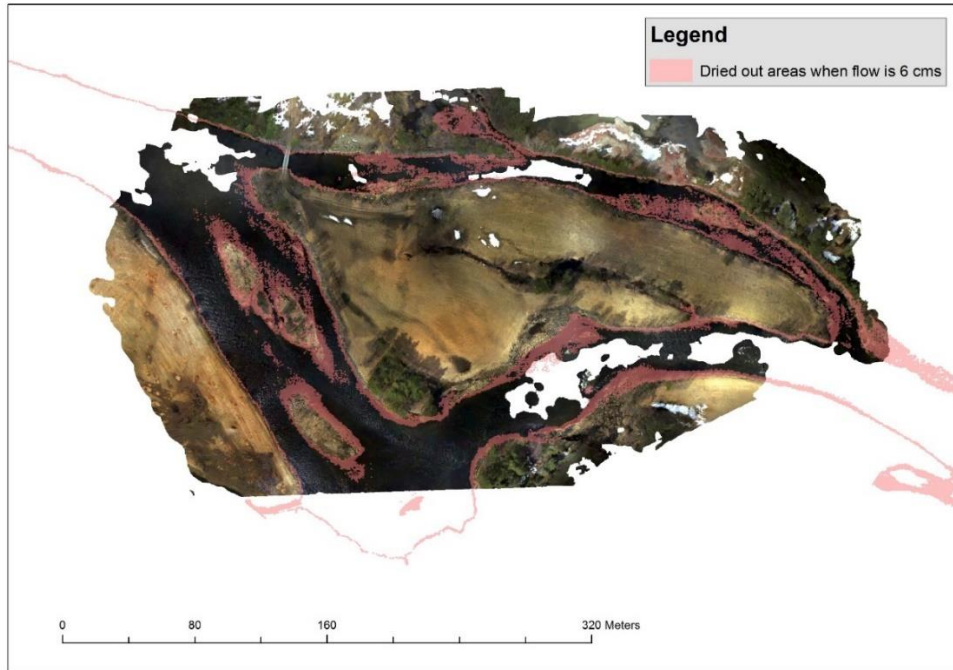


Figure D2. Gjerdeøyne island in Storåne with the dried-out areas when discharge is $6 \text{ m}^3/\text{s}$. Picture taken with Drone DJI Phantom 3 the May 9th, 2018

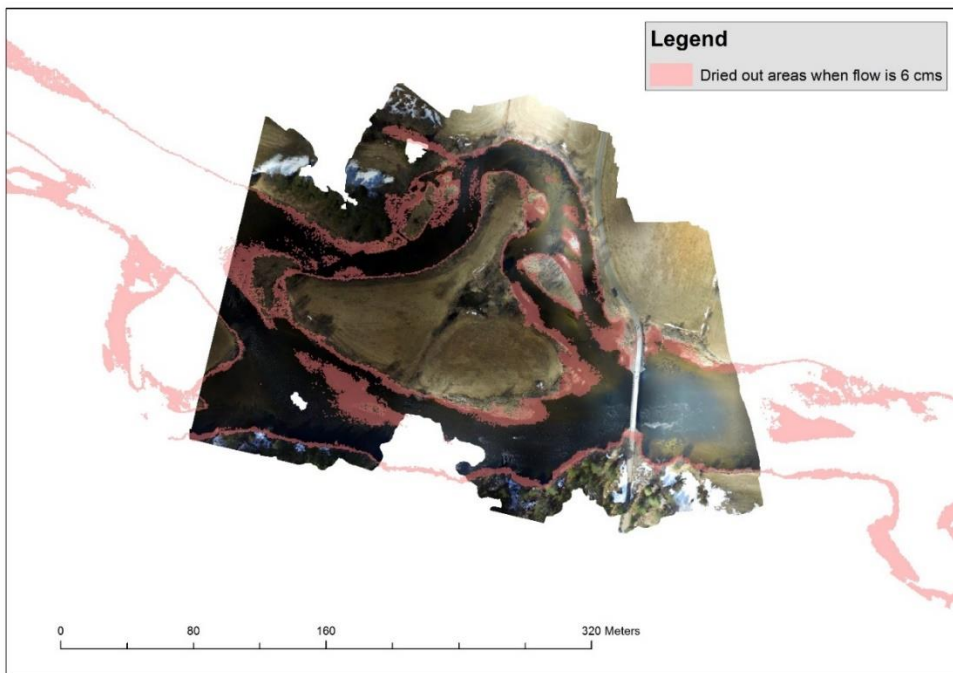


Figure D3. Morkaøyne island in Storåne with the dried-out areas when discharge is $6 \text{ m}^3/\text{s}$. Picture taken with Drone DJI Phantom 3 the May 9th, 2018

Appendix E Consideration of damping effect

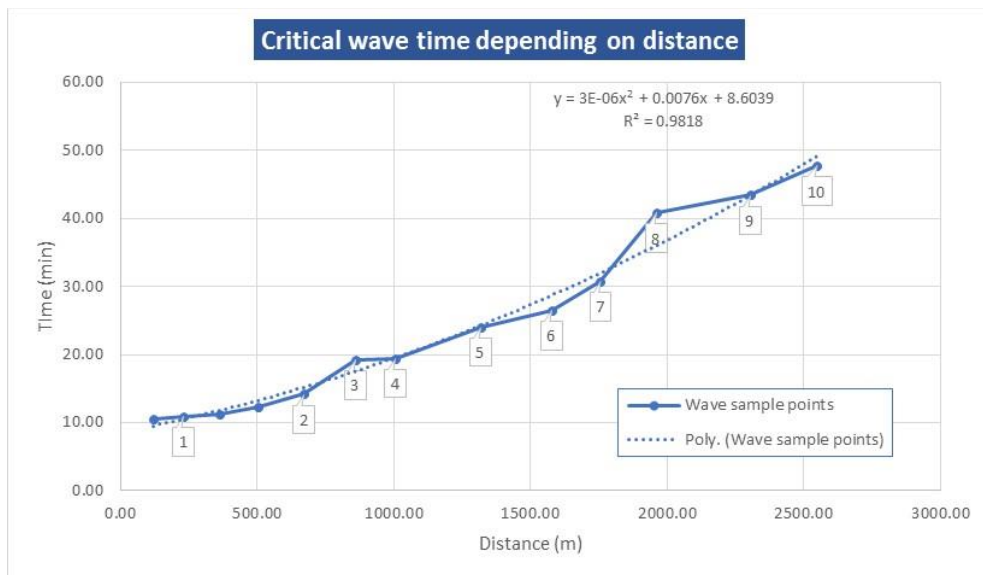


Figure E1. Critical time duration of the wave depending on the distance to the outlet in along Storåne

Appendix E Dewatering maps

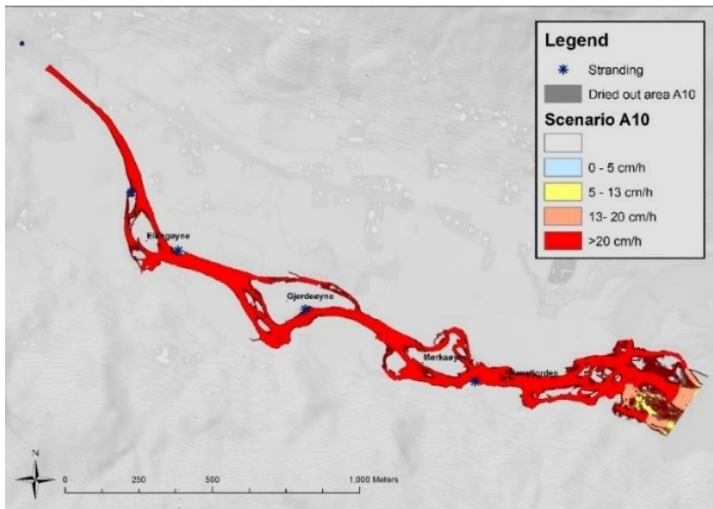


Figure F1. Dewatering rate in scenario A10

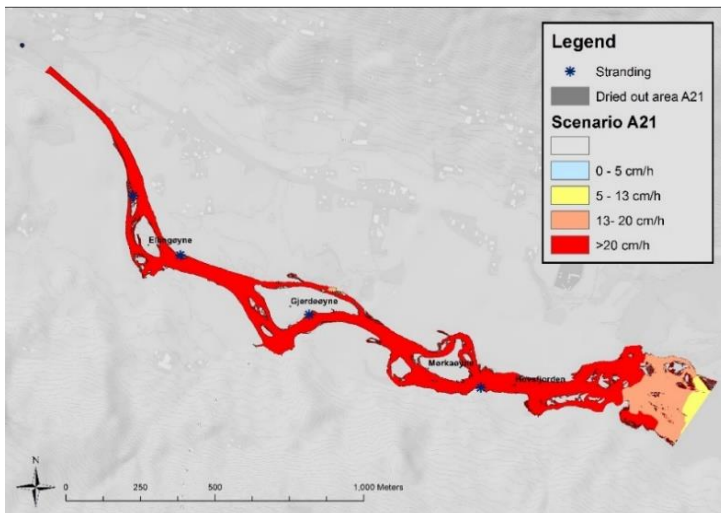


Figure F2. Dewatering rate in scenario A21

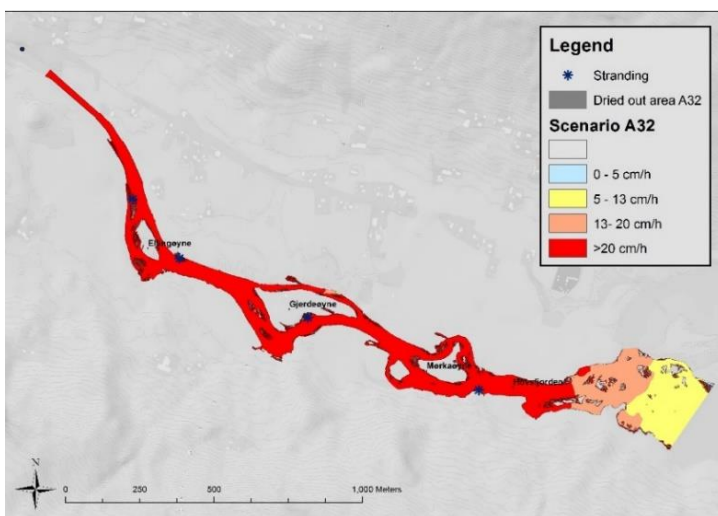


Figure F3. Dewatering rate in scenario A32

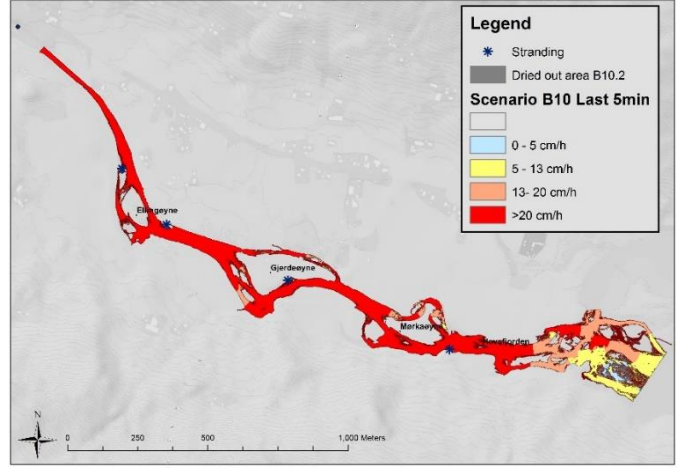
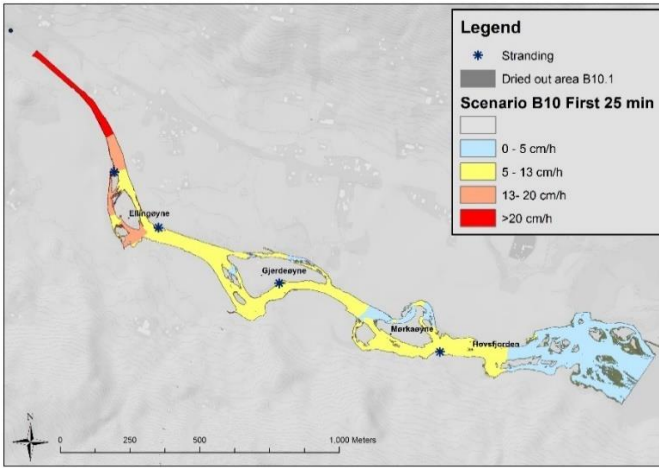


Figure F4. Dewatering rate in scenario B10 First 25 min and last 5 min

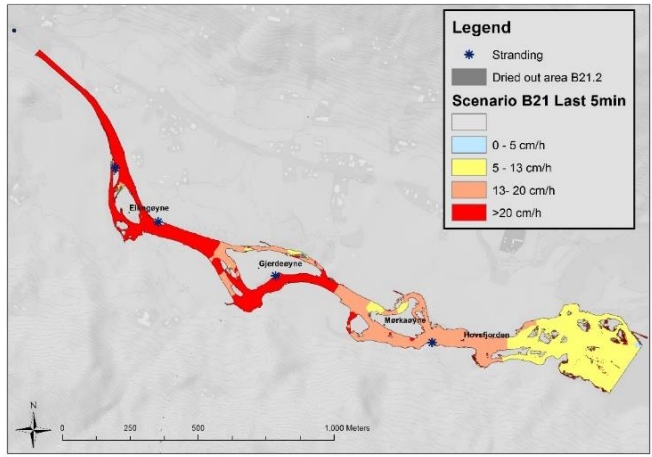
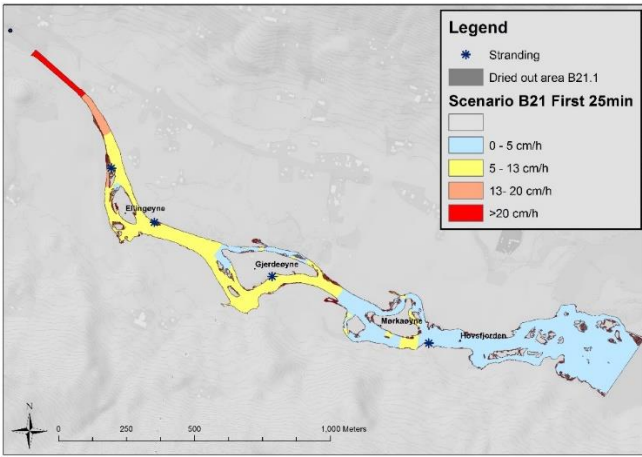


Figure F5. Dewatering rate in scenario B21 First 25 min and last 5 min

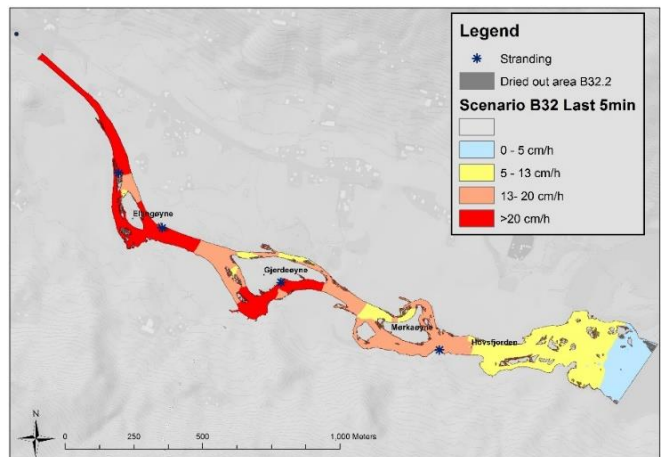
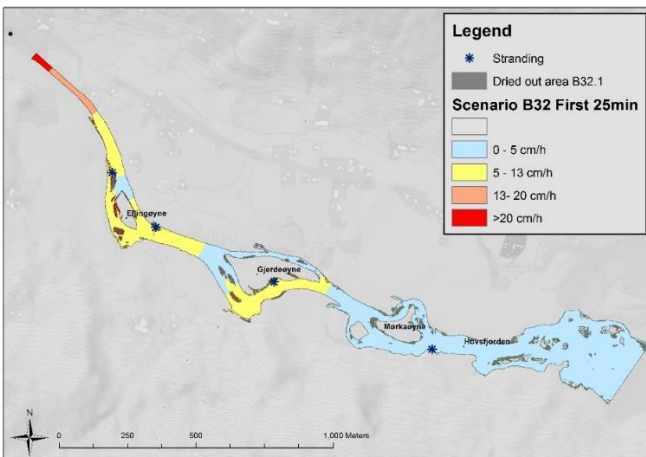


Figure F6. Dewatering rate in scenario B32 First 25 min and last 5 min

Shutdown time impact in dewatering velocity

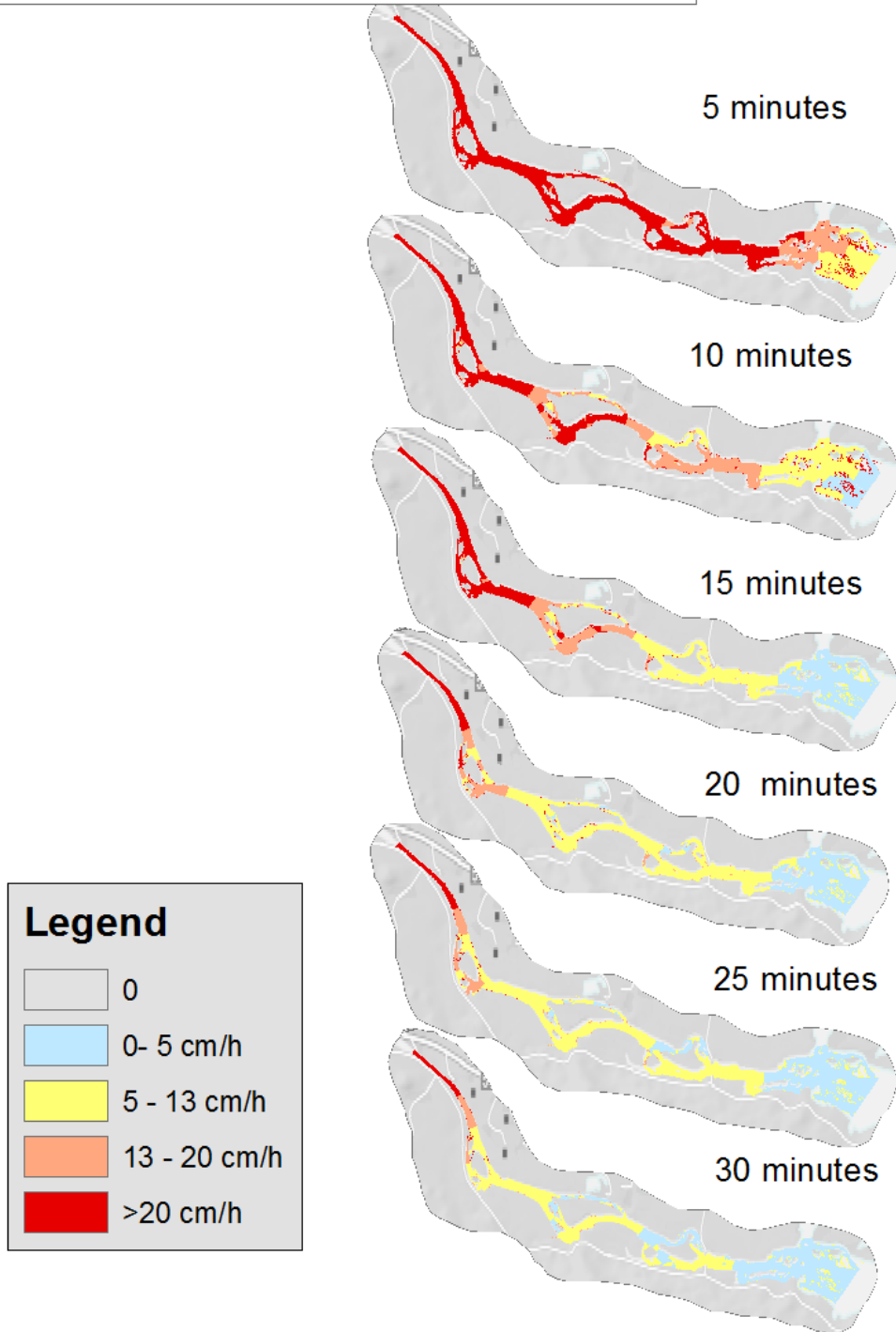


Figure F7. Dewatering rate for different time operation shut down

Appendix F Field pictures



Figure G1. Outlet and channel



Figure G2. Picture Ellingøyne from upstream. Indicated the western stream in Elligøyne, as potential location to take mitigation measurements.



Figure G4. Elligøyne from south. Indicated the western stream in Elligøyne, as potential location to take mitigation measurements.



Figure G5. Gjerdeøyne from downstream. Indicated the northern stream in Gjerdeøyne, as potential location to take mitigation measurements.



Figure G6. Gjerdeøyne from upstream Indicated the northern stream in Gjerdeøyne, as potential location to take mitigation measurements.



Figure G7. Gjerdeøyne from south



Figure G8. Mørkaøyne from upstream



Figure G9. Mørkeøyne from south

Appendix G Substrate distribution in Storåne

In the table S1, S5, S6, S8, S11 & S13 have more than 80% of substrate over 2 cm (coarser) and less of 5 % of fines. Notice that S11 and S6 correspond to the surroundings of Ellingøyne and the northern stream of Gjerdeøyne (Figure H2), both areas considered of high impact by hydropeaking operations.

Table G1. Percentage distribution of substrate

| St. | Prosentvis fordeling av substrat (mm) | | | | | Gjenklogging | Dekningsgrad (%) | | Rundhet | Vannhastighet | Middeldyp (cm) | Meso-habitat |
|-----|---------------------------------------|------|--------|---------|------|--------------|------------------|------|---------|---------------|----------------|--------------|
| | <2 | 2-20 | 20-100 | 100-250 | >250 | | Mose | Alge | | | | |
| S1 | 5 | 10 | 30 | 40 | 15 | 2-1 | 2-1 | 0 | KR | M/L | 100 | D |
| S2 | 10 | 30 | 45 | 10 | 5 | 2 | 2-1 | 0 | KR | M | 50 | B1 |
| S3 | 15 | 30 | 20 | 25 | 10 | 1-2 | 1-2 | 0 | KR | M/L | 130 | C |
| S4 | 20 | 40 | 40 | 10 | 0 | 2-1 | 2 | 0 | KR | M | 40 | B2 |
| S5 | 5 | 10 | 35 | 30 | 20 | 2 | 1-2 | 0 | KR | M/S | 70 | G2 |
| S6 | 5 | 15 | 35 | 35 | 10 | 2 | 2 | 0 | KR | M | 70 | B2/G1 |
| S7 | 15 | 30 | 20 | 25 | 10 | 2 | 1-2 | 0 | KR | L | 130 | C |
| S8 | 5 | 10 | 35 | 30 | 20 | 2 | 1 | 1 | KR | L | 70 | G2 |
| S9 | 20 | 20 | 20 | 25 | 5 | 1-2 | 2-3 | 0 | KR | L | 50 | D |
| S10 | 15 | 30 | 20 | 25 | 10 | 2 | 1-2 | 0 | KR | L | 150 | C |
| S11 | 5 | 10 | 10 | 45 | 30 | 1 | * | 0 | KR | S | 70 | G2 |
| S12 | 25 | 25 | 10 | 35 | 5 | 1-2 | 1-2 | 0 | KR | L/M | 50 | B1/D |
| S13 | 5 | 5 | 15 | 30 | 45 | * | * | * | KR | S | * | B1/G1 |

Tabellen oppsummerer de fysiske forholdene i Storåne nedstrøms utløpet fra Hol1 til Hovsfjorden (vannføring på ca. 30 m³/sek). Elva er delt i 13 hensiktsmessige soner der dominerende fordeling av bunnssubstrat, gjenklogging, dekningsgrad (mose/alge), rundhet, vannhastighet, middeldyp er beskrevet. Stjerne (*) = ikke undersøkt.

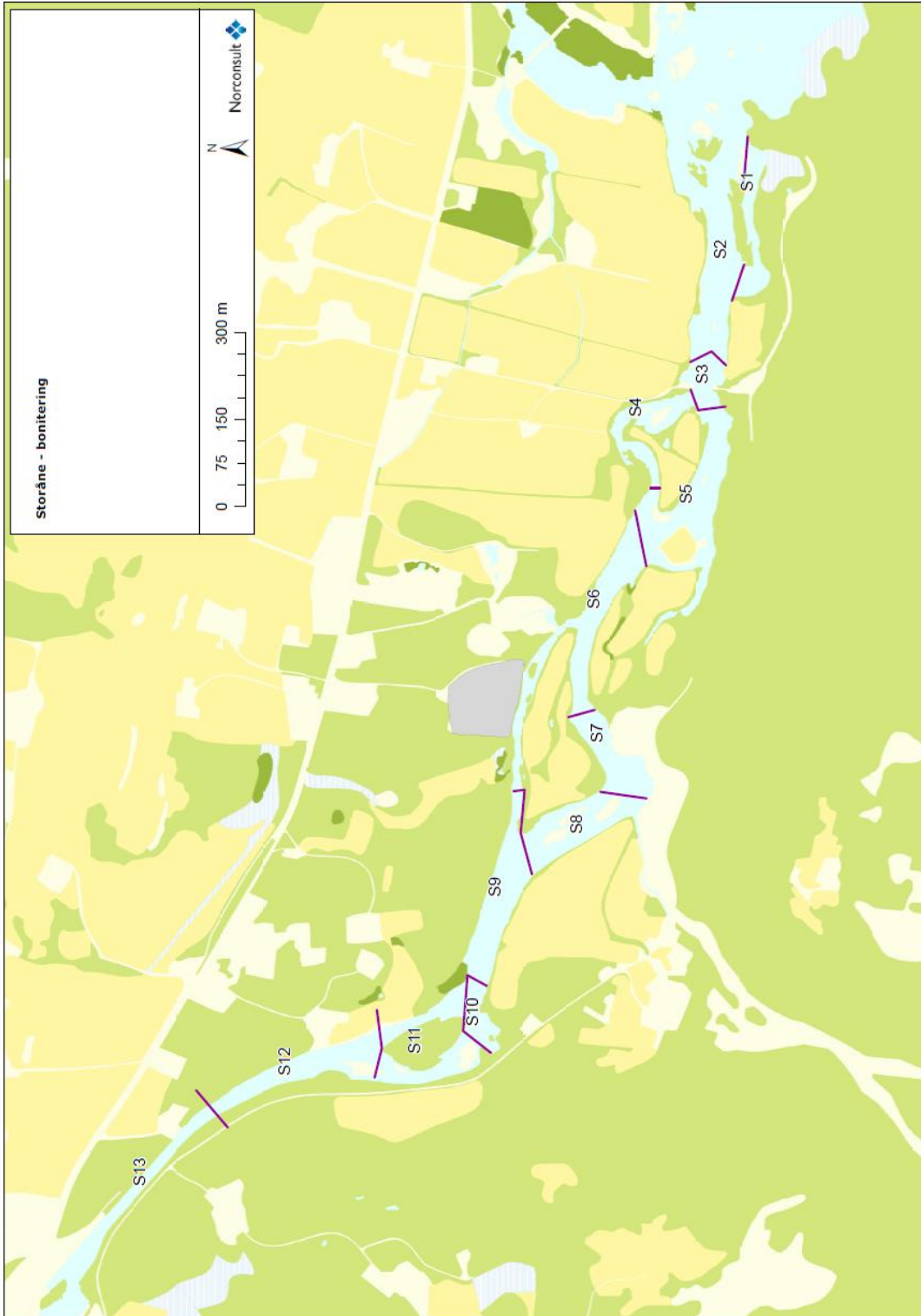


Figure G2. Sections in substrate study

Appendix H Fish density

Notat: Tetthet av ørret i Storåne i september 2016.

Svein Jakob Saltveit og Åge Brabrand

Innledning

Etter avtale med Bjørn Otto Dønnum er det gjennomført elektrofiske på til sammen 8 stasjoner i Storåne i september 2016. Stasjonene er de samme som er benyttet i tidligere undersøkelser av andre institusjoner.

Stasjonene ble overfisket tre ganger på oppmålt areal og tettheten av fisk ble beregnet ut fra avtak i fangst (successive removal) (Zippin 1958, Bohlin et al. 1989). I beregningene av tetthet av ørret er det skilt mellom årsunger (0+) og eldre ungfisk ($\geq 1+$), mens det for ørekyt ikke er skilt på årsklasser. Tetthet er oppgitt som antall fisk pr. 100 m², og er beregnet for alle enkeltstasjoner. Nedenfor HOL1, ble fisket gjennomført på stigende vannføring grunnet produksjonsstart i kraftverket.

Resultater og kommentarer

Tettheten av ørret og ørekyt er vist i Tabell 1. Det ble bare påvist ørekyt på stasjon R3 og S5, begge steder i svært lave tettheter. På berørt strekning nedenfor kraftverket ble ørret ikke påvist på stasjon S1 og S3. Eldre ørret ble bare funnet på stasjon S2 og S5, begge steder i svært lav tetthet. Årsunger (0+) var til stede i rimelige tetthet på S2, mens tetthetene var svært lave på S4 og S5. Tettheten av ørret, både 0+ og eldre, var betydelig høyere på referansestasjonene. Tetthet av årsunger av ørret var høy på de to øverste referansestasjonene, men lav på R3 pga. grovt substrat.

Fisket ble utført på stigende vannføring pga. drift i HOL1, og det er sannsynlig at fiske nedenfor utslippsstedet ble gjort på nylig vanndekket bunn. Unntaket her er trolig S2, der bratt elvebredd kan ha medført at det ble fisket på permanent vanndekket bunn, eller at bratt elvebredd har medført kort avstand mellom permanent og nylig vanndekket elveareal, og at ørret raskt kan kolonisere områdene nær land. For øvrig er det store bildet slik at det totalt sett er svært lave tettheter av ørret nedenfor utslippsstedet, mens de er betydelig høyere ovenfor. Det må understrekes at dette særlig gjelder eldre ørret.

Tabell 1. Beregnet tetthet (N/100m²) av ørret og ørekyt på tre stasjoner ovenfor HOL1 (R1-R3), og fem stasjoner nedenfor HOL1 (S1-S5) i Storåne, Hol kommune i september. P= fangbarhet.

| Stasjon | Areal m ² | Årsunger (0+) | | Eldre | | Ørekyt |
|---------|----------------------|---------------------|------|---------------------|------|---------------------|
| | | N/100m ² | p | N/100m ² | p | N/100m ² |
| R1 | 77 | 42,6 | 0,33 | 30,1 | 0,54 | 0 |
| R2 | 120 | 23,6 | 0,57 | 4,3 | 0,65 | 0 |
| R3 | 60 | 1,7 | 0,99 | 10,0 | 0,85 | 1,7 |
| S1 | 100 | 0 | | 0 | | 0 |
| S2 | 114 | 14,6 | 0,54 | 1,8 | 0,99 | 0 |
| S3 | 152 | 0 | | 0 | | 0 |
| S4 | 130 | 3,1 | 0,78 | 0 | | 0 |
| S5 | 132 | 3,8 | 0,82 | 1,5 | 0,99 | 0,8 |

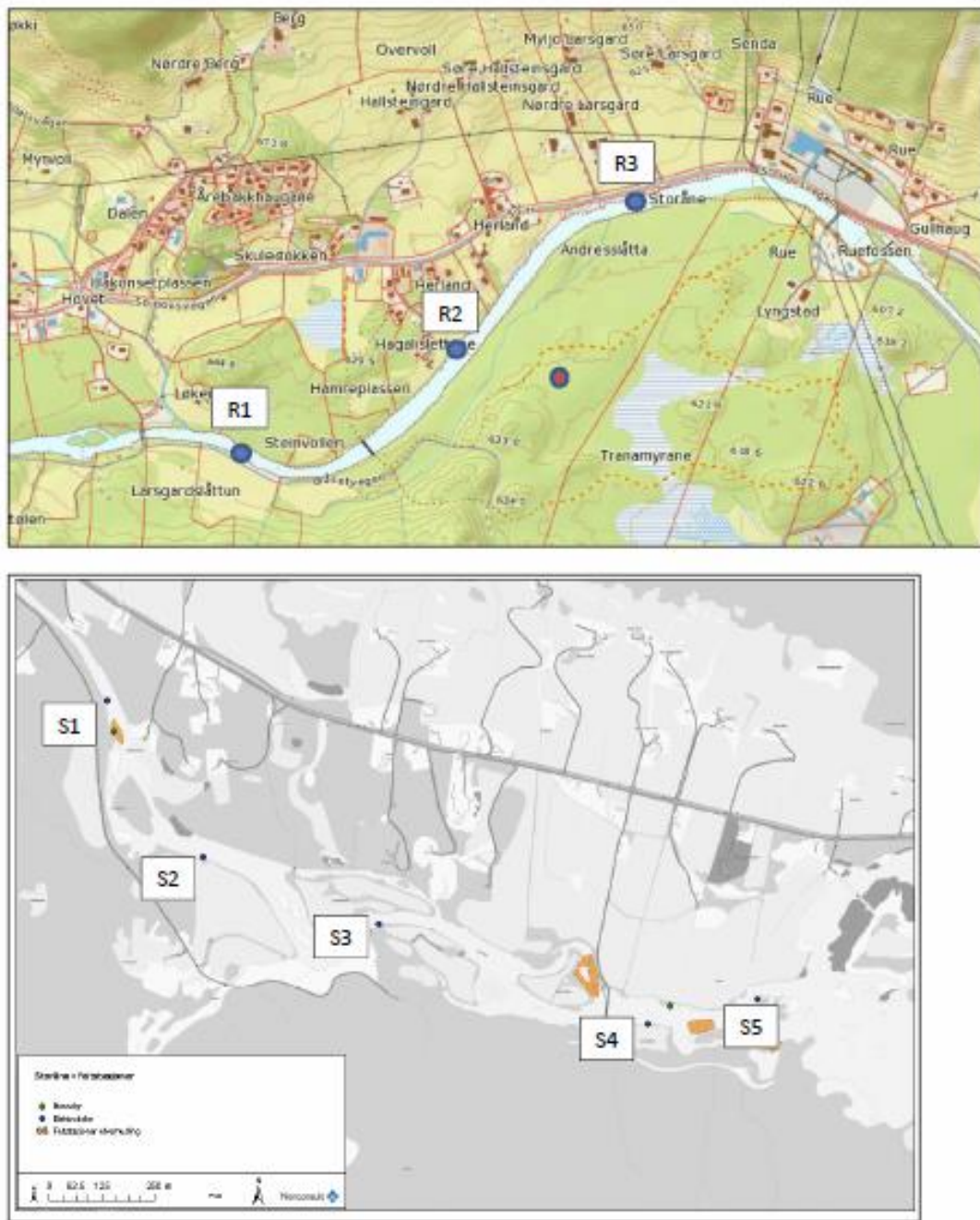


Fig. 1. Plassering av stasjoner for elektrofiske i Storåne i september 2016.

Appendix I Turbine restrictions

Hol I Operation limitations for the different turbines



For both sets of turbines we have a restriction on stopping the power plants during winter due to risk of freezing in the penstock.

The turbines must not operate at values under 40% of max discharge, as this is the limit set by the manufacturer of the turbines.

The machines do also operate under a regime controlled by Statnett and we are not free to start and stop the turbines always. This regime will set limitations for what is possible and might lead to scenarios that are not realistic.

Another important aspect when doing simulations are the costs of imposing a delayed ramping rate from maximum to zero capacity in let's say 20 minutes instead of the way we operate the machines today which is normally 5minutes from 0 to 100%.

A delayed ramping rate could also complicate our production planning, if a delay in delivered effect is carried over from hour x to hour x+1.

Table I1 Technical details:

| | HOL 1 Urunda | HOL 1 Votna |
|---|--|---|
| Turbines | 2 x 53 MW vertical Francis (machine no 3 and 4) | 2 x 57 MW vertical Francis (machine no 1 and 2) |
| Max discharge | 16.2 m ³ /s | 15.7 m ³ /s |
| Generator | 2 x 60 MVA | 2 x 65 MVA |
| Head | 380-352 m | 407-399 m |
| Reservoir capacity | Stradevatn-619.8 million m ³ | 4 different reservoirs-229.7 million m ³ |
| Energy factor | 0.897 kWh at 100% discharge | 1.0017 at 100% discharge |
| Most efficient operating discharge | 14.5 m ³ /s | 15 m ³ /s |

Ramping rate scenarios:

After running different scenarios in HEC-RAS using different starting points (up-down ramping with only discharge from upstream catchment, up-down ramping when we already have one turbine running... etc.) it should be possible to evaluate the possible effects on the environment in Storåne from varying discharge.

Med vennlig hilsen
E-CCO Energi AS
Bjørn Otto Dønnum
Fagsjef miljø

Appendix J Cost of changing operation

Changing the operational with a delayed in the ramping rate to 30 minutes will have a cost for the operator. The cost of changing the ramping rate for one turbine has been calculated assuming an energy price of 36 øre/KWh. We calculate the water that is spilled in the extra time of the scenario, assume an average number of decreases of 320 per year according to the COSH Tool analyze.

Table J1. Cost assumptions

| | | |
|----------------------------|---------|----------------------|
| Energy price | 36 | øre/kWh |
| Spilled water | 14400 | m ³ /day |
| Number of decreases | 320 | year |
| Spilled water | 4608000 | m ³ /year |

Table J2. Cost calculation for Hol I Urunda & Hol I Votna

| | HOL 1 Urund. | HOL 1 Votna | |
|-------------------------|---------------------|--------------------|----------------------|
| Energy factor | 0.897 | 1.0017 | kWh/m ³ |
| Energy of spilled water | 4133376 | 4615833.6 | kWh/year |
| Price | 1.5 | 1.7 | mill.NOK/year |

Appendix K Gol, Hallingdal river

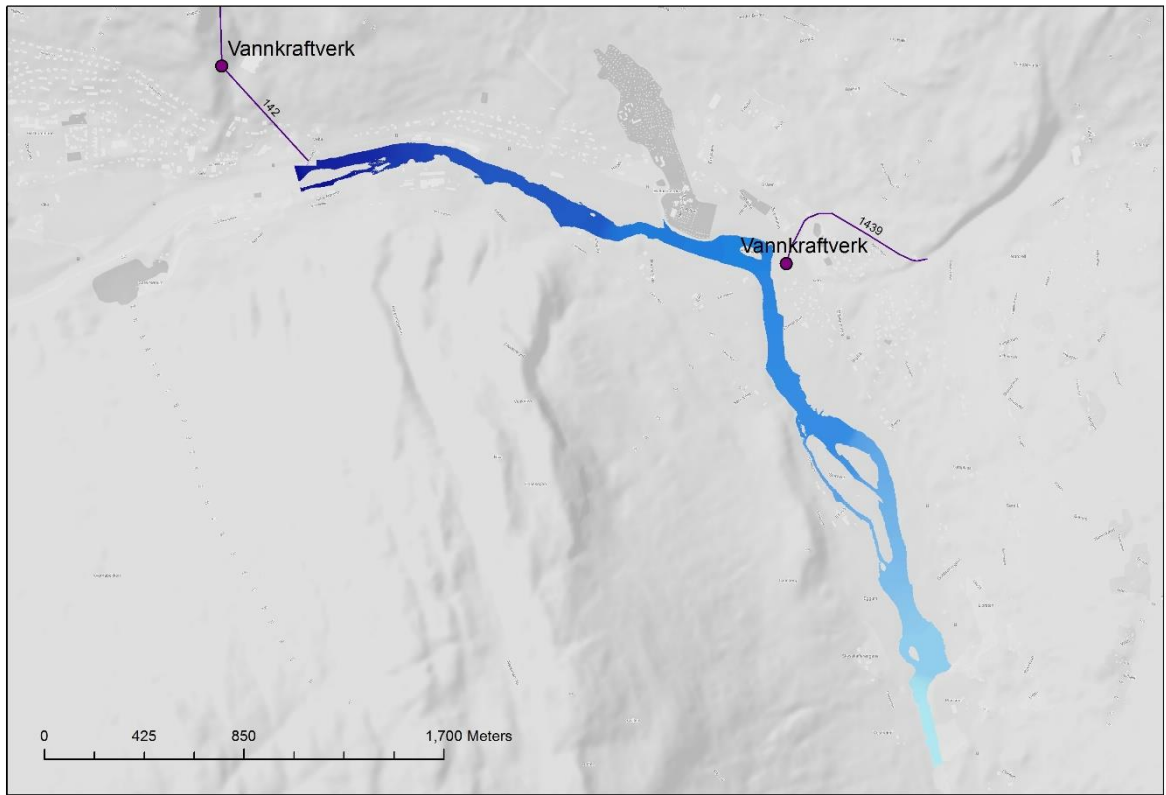


Figure K1 Simulation in Gol with HEC RAS for $Q=30 \text{ m}^3/\text{s}$